pubs.acs.org/acschemicalbiology

Articles

Orthogonal Active-Site Labels for Mixed-Linkage endo-β-Glucanases

Namrata Jain, Kazune Tamura, Guillaume Déjean, Filip Van Petegem, and Harry Brumer*

Cite This: https://doi.org/10.1021/acschembio.1c00063

Read Online

ACCESS | Metrics & More | Article Recommendations | Supporting Information

ABSTRACT: Small molecule irreversible inhibitors are valuable tools for determining catalytically important active-site residues and revealing key details of the specificity, structure, and function of glycoside hydrolases (GHs). β-glucans that contain backbone $\beta(1,3)$ linkages are widespread in nature, e.g., mixed-linkage $\beta(1,3)/\beta(1,4)$-glucans in the cell walls of higher plants and $\beta(1,3)$glucans in yeasts and algae. Commensurate with this ubiquity, a large diversity of mixed-linkage endoglucanases (MLGases, EC 3.2.1.73) and endo-$\beta(1,3)$-glucanases (laminarinases, EC 3.2.1.39 and EC 3.2.1.6) have evolved to specifically hydrolyze these polysaccharides, respectively, in environmental niches including the human gut. To facilitate biochemical and structural analysis of these GHs, with a focus on MLGases, we present here the facile chemo-enzymatic synthesis of a library of active-site-directed enzyme inhibitors based on mixed-linkage oligosaccharide scaffolds and *N*-bromoacetylglycosylamine or 2-fluoro-2-deoxyglycoside warheads. The effectiveness and irreversibility of these inhibitors were tested with exemplar MLGases and an endo-$\beta(1,3)$-glucanase. Notably, determination of inhibitor-bound crystal structures of a human-gut microbial MLGase from Glycoside Hydrolase Family 16 revealed the orthogonal labeling of the nucleophile and catalytic acid/base residues with homologous 2-fluoro-2-deoxyglycoside and *N*-bromoacetylglycosylamine inhibitors, respectively. We anticipate that the selectivity of these inhibitors will continue to enable the structural and mechanistic analyses of β-glucanases from diverse sources and protein families.

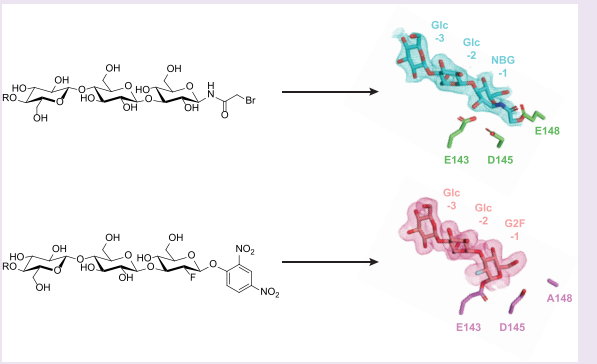

INTRODUCTION

Glycoside hydrolases (GHs) form the largest class of carbohydrate-active enzymes (CAZymes), currently consisting of over 165 sequence-based families.[1,2] Both reversible and irreversible inhibitors have aided in the biochemical and structural characterization of GHs, by enabling the elucidation of molecular details of active site-specificity and the identification of key catalytic residues.[3−6] Irreversible inhibitors, in particular, have been used in many studies to define the mechanisms of GH action and to reveal specific subsite recognition elements (see reviews[7−12] and recent primary literature[13−22]). Such knowledge is critical to inform mutational and evolutionary analysis, as well as guide enzyme engineering efforts to produce GHs with altered biochemical and biotechnological properties. When suitably modified by chromophores or affinity tags, irreversible inhibitors also find use in the labeling and identification of GHs in complex biological environments (reviewed in refs 12 and 23; for recent examples, see refs 24−26).

$\beta(1,3)/\beta(1,4)$-Glucans (mixed-linkage β-glucans, MLGs, Figure 1) are amorphous matrix polysaccharides found in the cell walls of cereals and other grasses, early diverging vascular and nonvascular plants, algae (seaweed), lichens, and some fungi.[27−31] MLGs are particularly abundant in oats and barley, in which they comprise ca. 70% of the soluble, nonstarch glycan content of the endosperm.[27,32] Thus, MLGs play major roles in plant cell wall structure and as a store of readily mobilized glucose for developing seedlings. The agricultural importance of MLGs is underscored by their direct contribution to human nutrition and health: MLG is an important component of the human diet and has been linked to reducing cholesterol and postprandial blood glucose levels.[32−34] In this context, the metabolism of MLGs is mediated by the gut microbiota,[35−38] which makes a significant contribution to the daily caloric intake in humans.[39] MLGs have also been of interest as a component of monocot feedstocks in large-scale bioethanol production.[28,30]

MLGs are composed predominantly of $\beta(1,4)$-D-glucopyranosyl linkages that are irregularly interspersed with $\beta(1,3)$ linkages (Figure 1), resulting in a kinked polysaccharide chain that resists crystallization.[28] In this sense, MLGs are distinguished from both cellulose ($\beta(1,4)$-glucan) and the all-β-(1,3)glucans that constitute major components of yeast and algal cell walls (e.g., laminarin), as well as the related plant callose and bacterial extracellular polysaccharides (e.g.,

Special Issue: Chemical Glycobiology

Received: January 29, 2021
Accepted: May 4, 2021

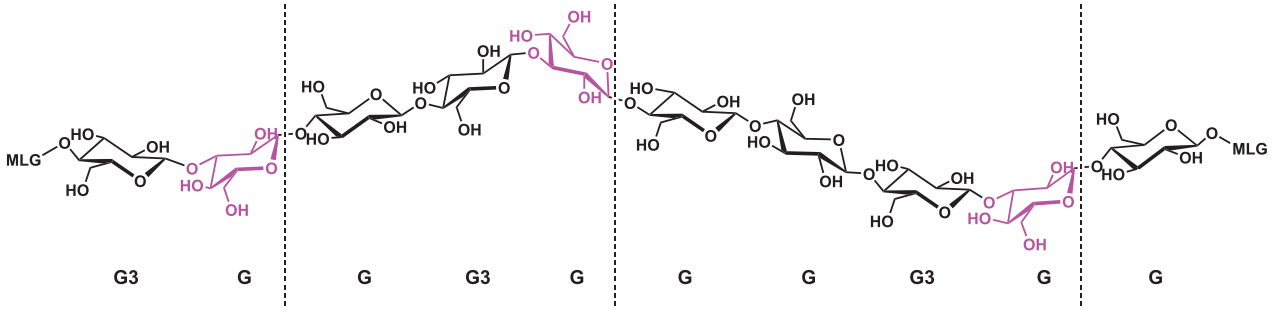

Figure 1. Representative structure of mixed-linkage β-glucan (MLG) from cereal crops and other grasses. **G** and **G3** indicate $\beta(1,4)$- and $\beta(1,3)$-linked glucosyl residues, respectively. The positions of polysaccharide chain hydrolysis by canonical bacterial mixed-linkage endoglucanases to yield oligosaccharides **GG3G** and **GGG3G** is indicated by dashed lines and magenta coloring.

Scheme 1. Mechanism of Anomeric-Configuration-Retaining Glycoside Hydrolases and Mechanisms of Inhibition: (a) Canonical Double-Displacement Glycoside Hydrolase Mechanism. (b) Mechanism of Inhibition by 2′,4′-Dinitrophenyl-2-deoxy-2-fluoroglycoside Inhibitors. (c) Mechanism of Inhibition by *N*-Bromoacetyl Glycosides

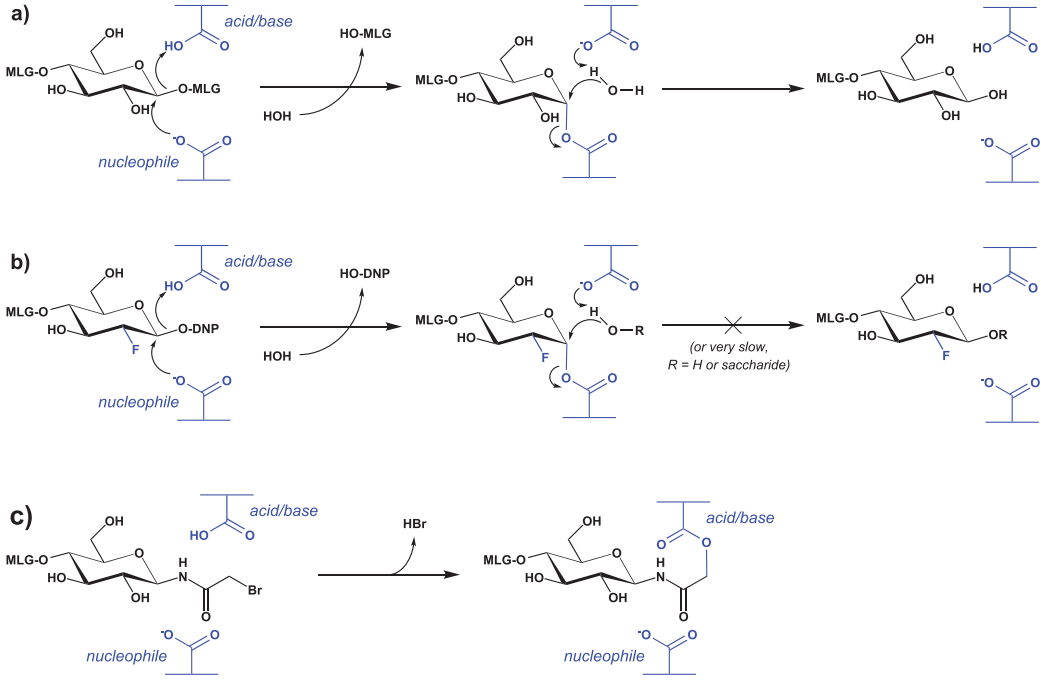

Curdlan).[40,41] The ratio of $\beta(1,4)$-Glc to $\beta(1,3)$-Glc residues in MLGs from different sources generally ranges from 2:1 to 3:1.[27] Although a small percentage of longer $\beta(1,4)$-linked stretches are present, the $\beta(1,3)$ linkages typically occur after every two or three β-(1,4)-linked residues. Thus, hydrolysis with specific MLGases, which cleave $\beta(1,4)$ linkages of 3-substituted Glc residues, results in a limit-digest comprised of **GG3G** and **GGG3G** (where "*G*" represents a glucosyl residue and "3" represents the position of the $\beta(1,3)$ linkage in the gluco-oligosaccharide, in the widely used shorthand nomenclature of MLG oligosaccharides).[a,27,35,42−44]

Because of the ubiquity of MLGs in nature, a broad diversity of GHs from archaea, bacteria, fungi, and plants has evolved to hydrolyze this family of polysaccharides. In addition to specific MLGases (EC 3.2.1.73; formally, $\beta(1,3)/\beta(1,4)$-D-glucan 4-glucanohydrolases, also known as licheninases), MLG can also be depolymerized by general *endo*-$\beta(1,4)$-glucanases (e.g., classic cellulases, EC 3.2.1.4), and *endo*-$\beta(1,3)$-glucanases (laminarinases, EC 3.2.1.39/EC 3.2.1.6). Specific MLGases are most commonly associated with Glycoside Hydrolase Family 16 (GH16; bacterial, fungal, and plant representatives)[43,45] and GH17 (plant representatives).[42] MLGase activity has also been found in members of the GH5,[44,46] GH6, GH7,[47] GH8, GH9,[48−50] GH11, GH12,[51] GH26,[52] and GH51 families (for an updated census by EC number, see http://www.cazy.org/Glycoside-Hydrolases.html; see ref 1), comprising both anomeric-configuration-retaining and configuration-inverting enzymes (Scheme 1).[53] In addition to their biological importance in carbohydrate metabolism,[28,35,42,43,54] MLGases have numerous biotechnological applications in biomass transformation to high-value products, in animal feed treatment to improve digestibility, in brewing to reduce mash viscosity, and for the preparation of defined prebiotics.[36−38,43,47,55,56]

Despite a long history of enzymological characterization,[43] including using bespoke aryl glycoside substrates,[57−59] there are few specific inhibitors for MLGases. These are essentially limited to nonhydrolyzable thio-oligosaccharide analogues as

https://doi.org/10.1021/acschembio.1c00063
ACS Chem. Biol. XXXX, XXX, XXX−XXX

Scheme 2. Synthesis of *N*-Bromoacetylglycoside Inhibitors

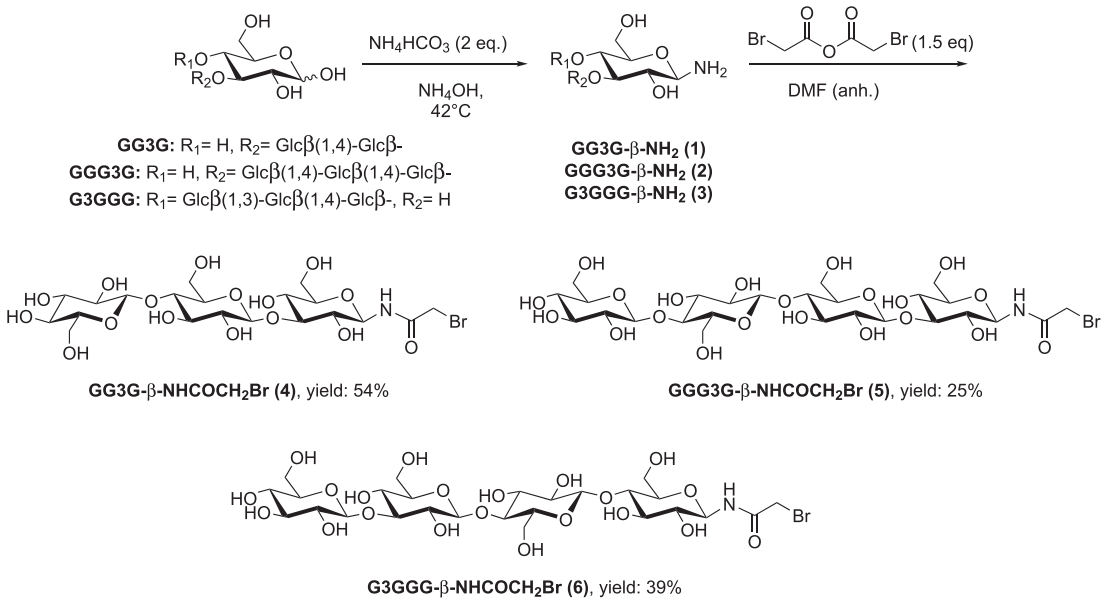

competitive (i.e., noncovalent, reversible) active site inhibitors.[60,61] On the other hand, epoxyalkyl-glucosides, epoxyalkyl-cellobiosides, epoxyalkyl-laminaribiosides, and epoxyalkyl-mixed-linkage oligosaccharides have been synthesized and tested as covalent inhibitors of MLGases, in some cases enabling the solution of enzyme-ligand complexes by X-ray crystallography.[20,62−64] Hence, there is significant scope for the development of novel covalent inhibitors of MLGases based on MLG oligosaccharide scaffolds. In the present study, we have focused our attention on the synthesis and application of MLGase inhibitors consisting of two distinct chemical warheads: 2-deoxy-2-fluoro glycosides[65] and *N*-bromoacetylglycosylamines (see Scheme 1).[66]

On one hand, 2-deoxy-2-fluoro glycosides (Scheme 1b) are well-established as inactivators of retaining glycoside hydrolases.[65,67,68] The replacement of the 2-OH in the natural glycone with fluorine eliminates key hydrogen-bonding interactions and inductively destabilizes the transition states leading to the formation and hydrolysis of the covalent glycosyl-enzyme intermediate. At the same time, a good leaving group at the anomeric position such as fluorine (HF, pK_a 3.2) or 2′,4′-dinitrophenyl (dinitrophenol, pK_a 4.1) enhances the rate of enzyme glycosylation, which results in kinetic trapping of the glycosyl-enzyme intermediate (Scheme 1b). Because they are still able to turnover by hydrolysis or transglycosylation, 2-deoxy-2-fluoro glycosides are essentially "slow substrates", with variable lifetimes of the corresponding glycosyl-enzyme intermediate, depending on the GH studied.[21,68−75] Nonetheless, these inhibitors have enjoyed widespread success for the specific labeling and identification of the catalytic nucleophile in retaining GHs from diverse families, because of their mechanistic mimicry.[8]

On the other hand, *N*-bromoacetylglycosylamines (Scheme 1c) consist of an electrophilic warhead appended to a carbohydrate as an enzyme specificity determinant. Displacement of bromine by nucleophilic residues such as active site carboxylates makes *N*-bromoacetylglycosylamines powerful probes to label and identify catalytic residues.[13,66,76−85] Despite their potential for off-target protein labeling,[44,86,87] mounting evidence suggests that *N*-bromoacetylglycosylamines exhibit specificity for the catalytic acid/base residues when productively bound by retaining glycosidases (Scheme 1c).[44,76,80,82,83,88]

Our group has recently reported the straightforward synthesis of *N*-bromoacetylglycosylamines and 2-deoxy-2-fluoroglycosides based on highly branched xyloglucan oligosaccharides as specific inhibitors of endoxyloglucanases.[13,21] A key feature of these syntheses was facile access to complex oligosaccharide building blocks through specific enzymatic hydrolysis of the parent polysaccharide, which obviated the need for tedious *de novo* synthesis. In the present study, we have extended this concept to produce a library of three *N*-bromoacetylglycosylamine and two 2-deoxy-2-fluoroglycoside inhibitors based on $\beta(1,3)/\beta(1,4)$-gluco-oligosaccharide scaffolds, which are readily obtained in multigram quantities as enzyme limit-digest products.[35,54,87] We also demonstrated the versatility of these inhibitors with exemplar GH16 MLGases and a GH158 laminarinase from the human gut microbiota using inhibition kinetics and intact protein mass spectrometry. Most notably, crystallography of covalent complexes with the *Bacteroides ovatus* MLGase *Bo*GH16 highlighted the ability of GG3G *N*-bromoacetylglycosylamine and 2-deoxy-2-fluoroglycoside congeners to orthogonally label the catalytic acid/base and nucleophile residues, respectively, in this retaining GH.

RESULTS AND DISCUSSION

Chemoenzymatic Syntheses of Candidate Inhibitors. The stereospecific and regiospecific synthesis of oligosaccharides is often laborious and fraught with challenges. Therefore, to rapidly access oligosaccharide building blocks of the target inhibitors, the commercially available polysaccharides laminarin and MLG were enzymatically hydrolyzed to yield the congeners **G3G**, **GG3G**, **GGG3G**, and **G3GGG** (see Scheme 2)[a] as starting materials for subsequent functionalization with reactive warheads. **G3G** was obtained by hydrolysis of algal laminarin with the broad-specificity β-glucanase, *Bu*GH16, from the human gut symbiont *Bacteroides uniformis*.[54] This

https://doi.org/10.1021/acschembio.1c00063
ACS Chem. Biol. XXXX, XXX, XXX−XXX

Scheme 3. Synthesis of 2-Deoxy-2-Fluoroglycoside Inhibitors

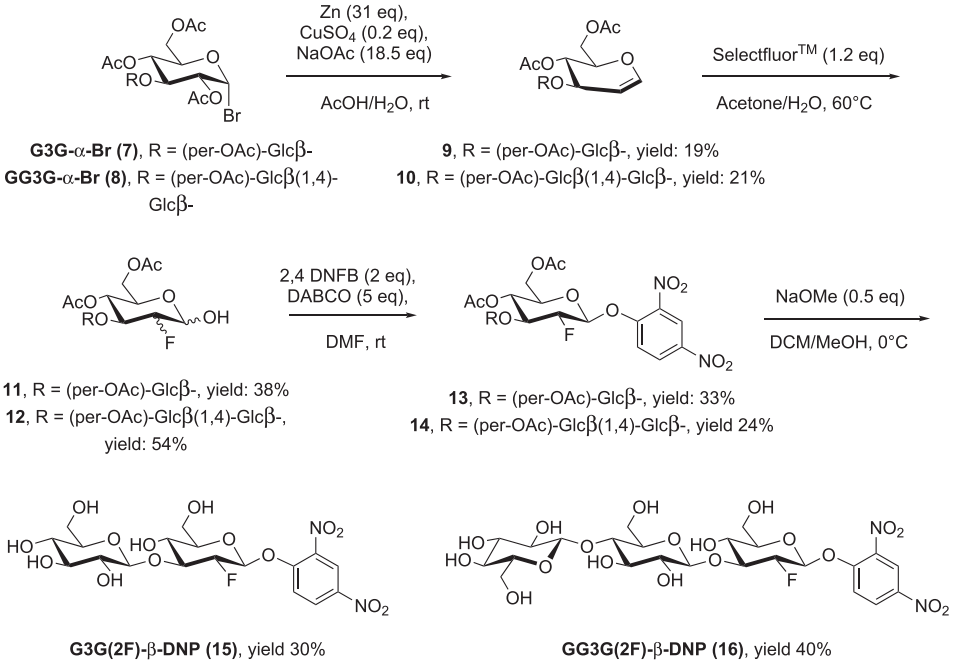

yielded a mixture of glucose, **G3G**, and a trisaccharide of undetermined structure,[54] which were readily separable via column chromatography after per-*O*-acetylation. Per-*O*-acetylated **GG3G** and **GGG3G** were likewise obtained in pure form from oat MLG, facilitated by the proficient MLGase, *Bo*GH16, from the human gut symbiont *Bacteroides ovatus*.[35] The tetrasaccharide (per-*O*-Ac)G3GGG, which differs from the aforementioned series by the position of the $\beta(1,3)$ linkage, was produced from oat MLG by employing the unique regiospecificity of the *Vitis vinifera* GH16 *endo*-glucanase.[87] Whereas the per-*O*-acetyl compounds allow direct entry into the synthetic routes for 2-deoxy-2-fluoro-glycoside inhibitors, straightforward Zemplen deprotection liberated the free oligosaccharides for *N*-bromoacetyl-glycosylamine syntheses.

To obtain the *N*-bromoacetyl glycosylamines, we applied and further optimized a two-step synthetic protocol[13,66,77,81] to install the electrophilic warhead (Scheme 2). Thus, **GG3G**, **GGG3G**, and **G3GGG** were aminated via dissolution in ammonium hydroxide and addition of ammonium bicarbonate at 42 °C (Scheme 2, compounds **1**−**3**). Here, an overnight (20 h) reaction time was sufficient, versus two-day reactions reported previously.[13,89] Conveniently, the use of unprotected oligosaccharides avoids additional, and potentially tedious, protection and deprotection steps. Following removal of the solvent and reagents under reduced pressure, amide formation using bromoacetic anhydride in dimethylformamide (DMF) was facile in all cases. The resulting *N*-bromoacetyl glycosamines were amenable to flash chromatography on silica gel to produce pure GG3G-β-NHCOCH$_2$Br (**4**, yield = 54%), GGG3G-β-NHCOCH$_2$Br (**5**, yield = 25%), and G3GGG-β-NHCOCH$_2$Br (**6**, yield = 39%) in moderate but sufficient yields.

On the other hand, the syntheses of the 2′,4′-dinitrophenyl-2-deoxy-2-fluoro-β-glycosides of **G3G** and **GG3G** from the corresponding per-*O*-acetates required a more extended synthesis, consisting of α-bromination, glycal formation, fluorination, glycosylation, and deprotection (Scheme 3). Thus, per-*O*-acetylated laminaribiose (**G3G**) and the MLG trisaccharide **GG3G** were converted to their respective α-glycosyl bromides **7** and **8**, using the standard treatment with HBr/HOAc[58,90] in excellent yields. Conversion to the respective glycals, **9** and **10**, with zinc powder[21] was also straightforward.

The incorporation of the 2-fluoro group in analogous 2-deoxy-2-fluoroglycosides has previously been achieved by electrophilic fluorination of per-*O*-acetylated glycals with acetyl or trifluoromethyl hypofluorite,[75,91,92] xenon fluoride,[93] or elemental fluorine.[94] More recently, these highly reactive and potentially hazardous reagents have been superseded by Selectfluor (1-chloromethyl-4-fluoro-1,4-diazoniabicyclo[2.2.2]octane bis(tetrafluoroborate))[95] for this purpose, because of its inexpensive commercial availability, ease of handling, high yields, and simultaneous introduction of a desired anomeric functional group.[96] However, the stereoselectivity of fluorine and hydroxyl group addition upon reaction with Selectfluor is dependent on various factors, including the specific configuration of the glycal, the nature of the hydroxyl protecting groups, and the choice of solvent and temperature.[97] In numerous previous examples, all four possible stereoisomers were obtained, yielding difficult-to-separate mixtures,[98−102] and additional anomeric acetylation or selective crystallization are often required.[75,103]

Such issues are potentially compounded in the synthesis of fluorinated oligosaccharides, in which the separation of such diastereomers becomes even more challenging. To avoid this problem, 2-deoxy-2-fluoro monosaccharides have previously been extended using trichloroacetimidate chemistry to obtain 2-deoxy-2-fluoro-disaccharide glycosides, such as 2,4-dinitrophenyl 4′-azido-2,4′-dideoxy-2-fluoro-β-xylobioside[104] and 2,4-dinitrophenyl 2-acetamido-2-deoxy-β-D-glucopyranosyl-(1,4)-2-deoxy-2-fluoro-β-D-glucopyranoside.[102] Similarly, specifically engineered glycosynthase enzymes have been used to extend the nonreducing end of monosaccharide inhibitors to yield the corresponding disaccharide and trisaccharide inhibitors.[105] On

https://doi.org/10.1021/acschembio.1c00063
ACS Chem. Biol. XXXX, XXX, XXX−XXX

Table 1. Apparent Inhibition Kinetics Parameters

inhibitor	enzyme	$k_{i\ (app)}$ (min^{-1})	$K_{i\ (app)}$ (mM)	$k_i/K_{i\ (app)}$ ($M^{-1}\ min^{-1}$)
GG3G-β-$NHCOCH_2Br$ (**4**)	*Bo*GH16	1.45 ± 0.27	1.68 ± 0.47	860
GGG3G-β-$NHCOCH_2Br$ (**5**)	*Bo*GH16	–	–	1920
G3G(2F)-β-DNP (**15**)	*Bu*GH158	0.087 ± 0.006	3.88 ± 0.624	22.4
GG3G(2F)-β-DNP (**16**)	*Bu*GH158	0.374 ± 0.018	3.12 ± 0.373	119

the other hand, we have previously been successful in stereoselectively 2-fluorinating a complex xyloglucan heptasaccharide (Xyl_3Glc_4, "XXXG") glycal with Selectfluor in the synthesis of an *endo*-xyloglucanase inhibitor,[21] which avoided tedious stepwise oligosaccharide construction.[106,107] Yet, prior to the present study, the use of Selectfluor on glycals containing $\beta(1,3)$ glycosidic linkages had not been explored.

Therefore, in an attempt to obtain exclusively the *gluco* epimer, small amounts (20 mg each) of **9** and **10** were subjected to electrophilic fluorination with Selectfluor in several precedented solvents (DMF, acetonitrile, nitromethane/H_2O, and acetone/H_2O mixtures). As exemplified by the laminaribiose (G3G) glycal (**9**), reactions using solvents with $MeNO_2$ or acetone yielded the *gluco* (α and β anomer) and *manno* (α anomer) epimers approximately in the same ratios (ca. 1:2; see Figure S1 in the Supporting Information). Reactions performed in DMF or acetonitrile yielded additional products, which were not further investigated, but were likely the result of solvent participation, as has been observed previously.[97,108] The absence of the *manno* β-anomer in all cases is consistent with previous reports[97,100,103] and can be rationalized by additive anomeric effects of the ring oxygen and axial 2-fluorine. Notably, in our previous work, the reaction of a highly branched xyloglucan heptasaccharide glycal afforded exclusively the *gluco* epimer with an anomeric α/β mixture (as confirmed by ^{19}F nuclear magnetic resonance (NMR) spectroscopy).[21]

Since we were unfortunately unable to bias the diastereoselectivity of fluorination here, the reactions of glycals **9** and **10** with Selectfluor were scaled-up using acetone/water (5:1) as a convenient solvent system to achieve moderate yields of diastereomeric mixtures. ^{19}F NMR spectra indicated that the diastereomeric ratios were similar to those observed in the small-scale reactions (**11**, Figure S27 in the Supporting Information; **12**, Figure S28 in the Supporting Information). Because of the difficulty in separating the three diastereomers obtained in each case as the free anomers, these mixtures were directly subjected to reaction with 2,4-dinitrofluorobenzene in the presence of DABCO. Upon workup, TLC of the crude product mixture showed three individual spots in each case. Purification using flash chromatography (toluene/acetone, 6.5:1) enabled the isolation of fractions corresponding to spots A2 (R_f = 0.47) and B2 (R_f = 0.38) as the desired β-*gluco* diastereomers, **13** and **14**, respectively, as ascertained by the ^{19}F NMR chemical shift and F−H spin coupling constants (see Figures S33 and S36, respectively, in the Supporting Information). Spots A1 (R_f = 0.40) and B1 (R_f = 0.34) correspond to α-*manno* diastereomers, while spots A3 (R_f = 0.55) and B3 (R_f = 0.47) correspond to the α-*gluco* diastereomers, respectively, as also concluded by ^{19}F NMR analysis (for ^{19}F NMR spectra and assignments of A1 and A3, see Figures S29 and S30, respectively, in the Supporting Information). Subsequent deprotection of **13** and **14** using Zemplen conditions and purification using flash chromatography yielded the target compounds G3G(2F)-β-DNP (**15**, yield = 30%) and GG3G(2F)-β-DNP (**16**, yield = 40%). The synthesis of the tetrasaccharide congener GGG3G(2F)-β-DNP was attempted but subsequently abandoned, because of an inability to separate a similar mixture of per-*O*-acetylated diastereomers of this longer oligosaccharide via flash chromatography.

Evaluation of Inhibitor Potency. *N-Bromoacetylglycosylamines.* To investigate their potency as inhibitors, the *N*-bromoacetylglycosylamines **4**, **5**, and **6** were incubated with an exemplar MLGase from glycoside hydrolase family 16,[45] *Bo*GH16.[35] A time- and concentration-dependent inactivation of the enzyme (8.9 μM) was observed upon incubation with GG3G-β-$NHCOCH_2Br$ (compound **4**; see Figure S2 in the Supporting Information) and GGG3G-β-$NHCOCH_2Br$ (compound **5**; see Figure S3 in the Supporting Information) at concentrations of 0.019−1.25 mM. At high concentrations of these compounds, the decline in enzyme activity was particularly rapid. Indeed, complete inhibition of the enzyme is apparent within the first 20 min of incubation of *Bo*GH16 with ≥0.156 mM of GGG3G-β-$NHCOCH_2Br$.

The covalent nature of the inhibition was demonstrated by intact-protein mass spectrometry after incubation of *Bo*GH16 with 2.5 mM of compounds **4** and **5**. In both cases, a 1:1 labeling stoichiometry is observed with no signs of overlabeling, as has been observed with *N*-bromoacetylglycosylamines in some cases.[13,66,77,80] Under identical concentrations of enzyme and G3GGG-β-$NHCOCH_2Br$ (compound **6**), there was no indication of labeling, even with extended incubation time (Figure S4 in the Supporting Information). These results are consistent with the known specificity of *Bo*GH16, which requires a $\beta(1,3)$ linkage spanning the −2 and −1 enzyme subsites[35] (subsite nomenclature according to ref 109).

Fitting of the Kitz−Wilson model[110] (see eqs 1−3 in the section titled "Materials and Methods") to the time- and concentration-dependent inhibition data obtained for GG3G-β-$NHCOCH_2Br$ (Figure S2) enabled the calculation of the apparent specific inhibition constants (eq 1, Table 1) and an apparent k_i/K_i value of 860 $M^{-1}\ min^{-1}$). These values compare favorably to those of other *N*-bromoacetylglycosylamine inhibitors, which similarly exhibit K_i values in the millimolar range.[13,44,77−79,81,83−85] However, the inactivation constants, k_i, for other *N*-bromoacetylglycosylamine inhibitors are 2−3 orders of magnitude lower.[13,44,77−79,81,83,85] The large error on the apparent K_i value, in this case, reflects an apparently poor ability to saturate the enzyme and a correspondingly flat k_{app} vs [I] curve (see Figure S2). Similarly, saturation inhibition kinetics were not achieved with the tetrasaccharide inhibitor GGG3G-β-$NHCOCH_2Br$ (compound **5**; see Figure S3 in the Supporting Information). Thus, a linear fit to the data was used to obtain an apparent k_i/K_i value of 1920 $M^{-1}\ min^{-1}$ (Table 1), which is comparable to that of the trisaccharide inhibitor GG3G-β-$NHCOCH_2Br$. As discussed in the protein structure section below, these results are concordant with the observation of three negative subsites in *Bo*GH16.[35]

https://doi.org/10.1021/acschembio.1c00063
ACS Chem. Biol. XXXX, XXX, XXX−XXX

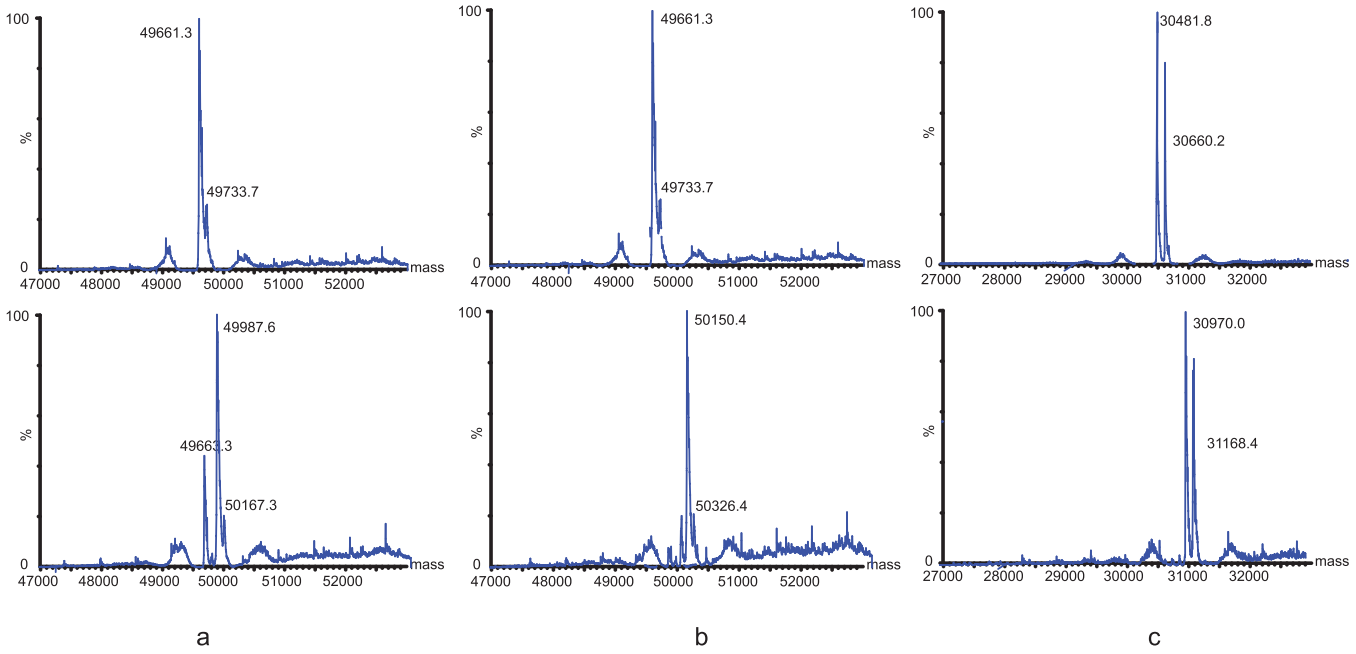

Figure 2. Stoichiometric labeling of β-glucanases with 2-deoxy-2-fluoroglycosides. Intact protein MS of wild-type enzymes before (upper panel) and after incubation with 2.5 mM 2-deoxy-2-fluoroglycoside for 2 h: (a) *Bacteroides uniformis* GH16 (*Bu*GH16) with G3G(2F)-β-DNP (**15**) (ΔM expected 327 Da), (b) *Bacteroides uniformis* GH16 (*Bu*GH16) with GG3G(2F)-β-DNP (**16**) (ΔM expected 489 Da), and (c) *Bacteroides ovatus* GH16 (*Bo*GH16) plus GG3G(2F)-β-DNP (**16**) (ΔM expected 489 Da). Phosphogluconoylation of each protein resulting from recombinant production in *E. coli* is observed at +178 Da.[137]

2′,4′-Dinitrophenyl-2-deoxy-2-fluoro-β-glycosides. Recently, our group elucidated the mechanism of laminarin digestion by a prominent member of the human gut microbiota, *Bacteroides uniformis*, with a particular focus on the structural and biochemical characterization of the GHs *Bu*GH158 and *Bu*GH16 encoded within a complex Polysaccharide Utilization Locus.[54] *Bu*GH158 was confirmed to be a highly specific anomeric configuration-retaining endo-β(1,3) glucanase with high activity on laminarin from *Laminaria digitata* (brown algae) and limited activity on MLG from barley (*ca.* 140-fold lower). *Bu*GH16 was found to be a broad-specificity endo-β(1,3)/β(1,4)-glucanase with activity on *L. digitata* laminarin ∼4 times higher than barley MLG.[54]

As a representative retaining laminarinase/MLGase, *Bu*GH158 was then used to study the potency of **15** and **16** as potential inhibitors, using the chromogenic substrate 2′-chloro-4′-nitrophenyl-β-laminaribioside (G3G-β-CNP) to measure residual activity (K_m = 12.6 ± 1.15 mM, k_{cat} = 1918 ± 154 min^{-1}; see Figure S5 in the Supporting Information). At concentrations ranging from 0.31 to 10 mM, both **15** and **16** exhibited a time- and concentration-dependent inactivation of *Bu*GH158 over 3 h, with rapid and complete inactivation by **16** being particularly apparent (see Figures S6 and S7 in the Supporting Information). Kitz−Wilson kinetic analysis (eqs 1−3) allowed the calculation of the apparent inhibition constants for **15** and **16** (Table 1). The apparent k_i values reported here are either in a similar range[75,111−115] or 1−2 orders of magnitude lower[65,68,70,72,116] than similar 2-deoxy-2-fluoro-dinitrophenyl or 2-deoxy-2-fluoro-glycosyl fluoride inhibitors. The apparent K_i values observed here are in a comparable millimolar range.

Intact-protein mass spectrometry of *Bu*GH158 upon incubation with 2.5 mM of **15** or **16** revealed the covalent nature of inhibition and stoichiometric labeling of the enzyme after 2 h (Figures S6 and S7). An increase in protein molecular weight of 325.8 and 488.0 Da, respectively, were observed for **15** and **16** upon incubation with the enzyme. These results are consistent with the addition of a single 2-deoxy-2-fluoro **G3G** moiety and a single 2-deoxy-2-fluoro **GG3G** moiety, respectively. No trace of the free enzyme was observed for either inhibitor, indicative of relatively stable glycosyl-enzyme intermediates with limited turnover over the course of the incubation. In comparison, the retaining MLGase *Bu*GH16 was labeled by **15** and **16** (Figure 2). However, labeling with **15** was incomplete, suggesting either slow inhibition or slow turnover.[73]

To exemplify the versatility of these inhibitors to label a range of β-glucanases, the mixed-function laminarinase/MLGase *Bu*GH16 and the MLGase *Bo*GH16 were both subjected to qualitative intact protein MS analysis following treatment with **15** and **16** for 2 h. Notably, *Bu*GH16 appeared to be incompletely labeled by G3G(2F)-β-DNP (**15**) during this period, but was completely labeled by GG3G(2F)-β-DNP (**16**). Similarly, complete labeling of the MLGase *Bo*GH16 was observed using **16** (Figure 2) as a prelude to subsequent crystallography.

Structural Analysis of Covalent Enzyme Complexes. To provide structural insight into the modes of inhibition, the complexes formed by the incubation of GGG3G-β-$NHCOCH_2Br$ and GG3G(2F)-β-DNP with *Bo*GH16 were solved to resolutions of 2.15 and 1.56 Å, respectively, via X-ray crystallography (Table S1 in the Supporting Information). The overall tertiary structure, comprising a canonical β-jelly roll fold typical of GH16,[45] was virtually identical to previously determined unliganded and GGG3G product−complexed structures of *Bo*GH16 (PDB IDs 5NBO and 5NBP, respectively[35]) (see Figure 3).

The GGG3G-β-$NHCOCH_2$ complex structure was successfully obtained by soaking crystals in a solution containing 2.5 mM of compound **5** (the same concentration used for intact

https://doi.org/10.1021/acschembio.1c00063
ACS Chem. Biol. XXXX, XXX, XXX−XXX

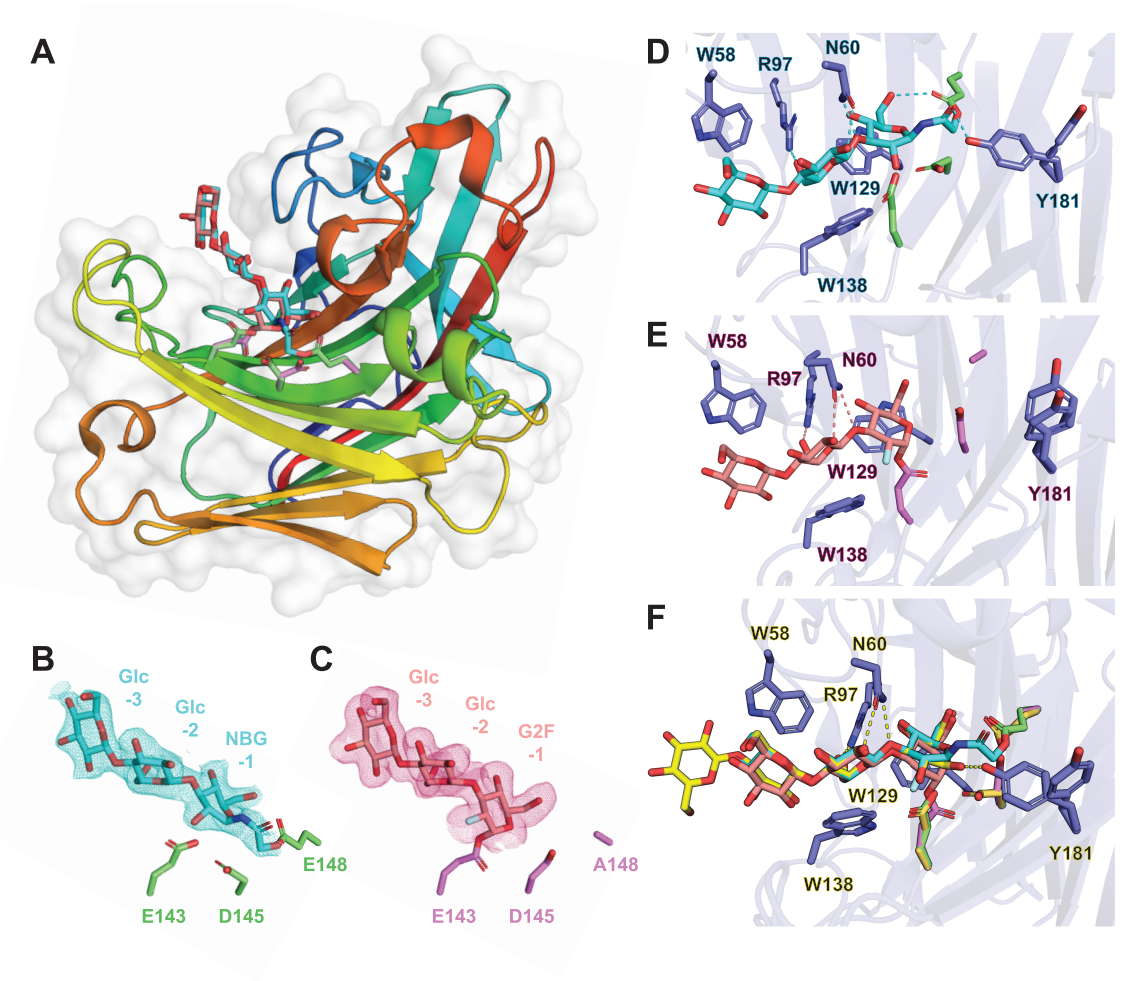

Figure 3. Crystal structure of *Bo*GH16-inhibitor complexes. (A) Overall structure with *Bo*GH16 shown in cartoon color ramped from blue (N-terminus) to red (C-terminus) with transparent surface in white. Both inhibitors bound in the active site are shown as sticks (GG3G-β-NHCOCH$_2$ in cyan and GG3G(2F) in rose throughout the figure), as are catalytic and other key active-site residues. (B) The F$_o$-F$_c$ omit density map (generated by Privateer[136]) of GG3G-β-NHCOCH$_2$ contoured at 3.0 σ. (C) The F$_o$-F$_c$ omit density map (generated by Privateer[136]) of GG3G(2F) contoured at 3.0 σ. (D) *Bo*GH16 active site interactions with GG3G-β-NHCOCH$_2$, with hydrogen bonds (3.0 Å or shorter) shown as cyan-colored dashed lines. (E) *Bo*GH16 E148A active-site interactions with GG3G(2F), with hydrogen bonds (3.0 Å or shorter) shown as rose-colored dashed lines. (F) Superposition of the two inhibitors and a **GGG3G** tetrasaccharide product (yellow sticks; PDB ID: 5NBP) in the *Bo*GH16 active site, with hydrogen bonds (3.0 Å or shorter) to **GGG3G** shown as yellow dashed lines.

protein MS experiments, which is 2-fold greater than the highest concentration used for kinetics experiments; see Figure S3). Notably, the observed electron density corresponding to the covalently bound inhibitor was superior in chain A. The lower occupancy observed in chain B was attributed to the proximity of the active site to a protein chain from a neighboring asymmetric unit. Nevertheless, the near-complete glycone was modeled into the active site of chain A, spanning subsites −1 to −3, including the *N*-acetylated glucosylamine residue in subsite −1 (see Figure 3b, as well as Table S2 in the Supporting Information). The observed electron density unambiguously revealed that the catalytic acid/base residue, Glu148, was labeled by nucleophilic substitution of the bromide (Figure 3d). Notably, the Glu148 side chain underwent a minor rotation and shift in orientation to accommodate the covalent linkage between Oε and *N*-acetyl group of the inhibitor (Figure 3). The density of the nonreducing-terminal glucosyl residue corresponding to subsite −4 was too poor to model (Figure 3b), reminiscent of the relatively high disorder of this residue in the *Bo*GH16:GGG3G product complex.[35]

The inhibitor complex structure clearly revealed that the β orientation of the *N*-bromoacetyl group distanced the electrophilic warhead away from the catalytic nucleophile Glu143, which is positioned directly below the anomeric carbon. Instead, the *N*-acetyl group filled the space that typically accommodates a water molecule in the glycosyl-enzyme intermediate of the normal catalytic cycle, which ideally positioned the electrophile for nucleophilic attack by Glu148. The natural role of this residue is to deprotonate a water molecule for turnover of the glycosyl-enzyme intermediate in the second step of the canonical double displacement GH mechanism (Figure 1)[53,117] The fact that the catalytic acid/base residue is labeled, rather than the catalytic nucleophile, is similar to previous observations with *N*-bromoacetylglycosylamine inhibitors.[44,76,80,82,83,88]

Despite extensive efforts, including screening various concentrations and soaking times, we were unable to obtain a GG3G(2F)-bound complex structure of wild-type *Bo*GH16,

https://doi.org/10.1021/acschembio.1c00063
ACS Chem. Biol. XXXX, XXX, XXX−XXX

because of the apparent turnover of the 2-deoxy-2-fluoroglycosyl-enzyme, which is a well-known phenomenon with some glycosidases.[73] Hence, we replaced the catalytic acid/base, Glu148, with an alanine to further retard the turnover of the inhibitor-enzyme complex.[73] Through this approach, we successfully captured the inhibitor-bound complex by soaking crystals of the E148A mutant in a solution containing 5 mM inhibitor for 20 min. Clear electron density corresponding to the inhibitor was observed in both molecules in the asymmetric unit, which allowed modeling of the complete trisaccharide spanning subsites −1 to −3 in both chains (see Figure 3b, as well as Table S3 in the Supporting Information). A covalent bond was clearly observed between C-1 and the catalytic nucleophile, Glu143, in the glycosyl-enzyme intermediate (Figure 3b, *cf.* Figure 1). Relative to the wild-type, Glu143 is rotated toward the "electrostatic helper", Asp145, which is widely conserved in GH16 members.[45] Asp145, in turn, is swung toward the space normally occupied by the side chain of Glu148. In wild-type *Bo*GH16, Glu143 likely assumes the normal, unrotated conformation in the covalent glycosyl-enzyme.

Other than the notable difference of labeling different catalytic residues, both inhibitors display essentially identical interactions with the *Bo*GH16 active-site cleft, including carbohydrate-aromatic stacking with Trp129 and Trp138 at the −1 and −2 subsites, respectively, as well as several hydrogen bonds (Figure 3). Except for the −1 subsite (*vide infra*), the individual Glc residues of both inhibitors superimposed closely with the GGG3G oligosaccharide in our previously solved product complex (PDB ID: 5NBP[35]) (Figure 3f). Interestingly, the same "swung in" rotamer of Tyr181 observed in the GGG3G product complex[35] is seen with the GGG3G-NHCOCH$_2$ inhibitor (Figure 3d, *cf.* Figure 3f). However, instead of making a hydrogen bond with the anomeric (C1) hydroxyl of the glucosyl residue in subsite −1 (Figure 3d), the hydroxyl group of Tyr181 hydrogen bonds to the carbonyl oxygen of the *N*-acetyl group of the inhibitor (Figure 3f). This mobile tyrosine did not assume a similar "swung in" position in the GG3G(2F) covalent complex, because of a lack of hydrogen bonding partner (Figure 3e).

A further notable difference between the inhibitors is that, in the GGG3G-β-NHCOCH$_2$−complex, the *N*-acetylated glucose in subsite −1 assumed a ^{4}E envelope conformation (Table S2), whereas the low-energy ^{4}C$_1$ chair conformation was observed in the GG3G(2F) complex (as well as the GGG3G product complex) (Figure 3). It appears that, due to geometric constraints of the Glu148 side chain position and the conservation of active site interactions, the anomeric carbon is pulled upward by the *N*-acetyl linkage to Glu148 (Figure 3d). Considering these observations together, the ^{4}E envelope conformation can be rationalized by a lower energy requirement to bring the sugar out of the relaxed ^{4}C$_1$ chair conformation than that needed to compromise the numerous interactions between the tetrasaccharide and the side chains that compose the enzyme active site.

CONCLUSION

In this work, the synthesis of active-site directed β-glucanase inactivators, which consist of mixed β(1,3)/(1,4) linkages as specificity determinants, was significantly enabled by ready access to the corresponding oligosaccharide building blocks via enzymatic hydrolysis of bulk polysaccharides. Indeed, to the best of our knowledge, this is the first report of the controlled synthesis of *N*-bromoacetylglycosylamines and 2-deoxy-2-fluoro glycosides containing β(1,3)-glycosidic linkages. Whereas the potency of these inhibitors was demonstrated through enzyme kinetic analysis and intact protein mass spectrometry, protein crystallography revealed that these two classes of inhibitors exhibit orthogonal specificity for the catalytic acid/base and catalytic nucleophile, respectively, of an exemplar mixed-linkage endoglucanase. Hence, deploying tandem pairs of *N*-bromoacetylglycosylamines and 2-deoxy-2-fluoroglycosides has significant scope in the mechanistic analysis of GHs. This work contributes to the active field of small-molecule covalent probes for GH characterization. We envision that these inhibitors could be elaborated into probes for activity-based protein profiling[8,9,23] by additional chemistry, including the use of glycosynthases to extend the glycone specificity element with reactive handles.[118] Furthermore, in light of recent renewed interest in covalent inhibitors as drugs,[119] such molecules could potentially be used to control microbial populations. Such applications will of course be dependent on the biological environment in which they are deployed, noting that 2-deoxy-2-fluoroglycosides generally have long hydrolytic half-lives (tens of days at 37 °C),[120] while *N*-bromoacetylglycosylamines may be prone to side reactions with nitrogen and sulfur nucleophiles.[44,66]

MATERIALS AND METHODS

Enzyme Sources. The *Vitis vinifera* (grape) *endo*-(xylo)glucanase variant *Vv*EG16 (ΔV152) was produced as previously described.[87] The *Bacteroides uniformis* laminarinase *Bu*GH158 and MLGase *Bu*GH16 were produced as previously described.[54] The *Bacteroides ovatus* MLGase *Bo*GH16 construct in pET28 vector (*Bo*GH16:-pET28) from a previous study was utilized for wild-type recombinant protein production.[35] The catalytic acid/base mutant *Bo*GH16 E148A was generated by site-directed mutagenesis, using the QuickChange (Agilent Technologies) protocol with PfuUltra high-fidelity polymerase (Agilent Technologies) and DpnI (New England Biolabs). PCR amplification was conducted using the forward primer 5′-GGG AGA TTG ATA TTA TGG CTA TGG GAG AAC AGA GCG-3′, reverse primer 5′-CGC TCT GTT CTC CCA TAG CCA TAA TAT CAA TCT CCC-3′, and the *Bo*GH16:pET28 plasmid as the template. Successful generation of clones and site-directed mutants was verified by Sanger sequencing (Genewiz).

Recombinant *Bo*GH16 and the *Bo*GH16 E148A mutant were produced in *E. coli* BL21 (DE3) and purified by nickel affinity chromatography as described previously,[35] with the exception that HEPES buffers were used instead of sodium phosphate (binding buffer: 20 mM HEPES pH 7.4, 500 mM sodium chloride, 20 mM imidazole; elution buffer: 20 mM HEPES pH 7.4, 500 mM sodium chloride, 500 mM imidazole). The protein used in crystallography was further purified by size exclusion chromatography, using Superdex 75 (GE Healthcare) packed in XK 16/100 column (GE Healthcare) run with 10 mM HEPES pH 7.0. The fractions were inspected for purity by SDS-PAGE and pure fractions were pooled and concentrated in Vivaspin centrifugal filters (GE Healthcare). Final protein concentration was determined by spectrophotometry at 280 nm in an Epoch Microplate Spectrophotometer (BioTek) using the extinction coefficient 54 890 M^{-1} cm^{-1}, which was calculated from the primary sequence using ProtParam tool from the ExPASy Bioinformatics Resource Portal.[121]

Inhibitor Synthesis. *General.* All reagents were analytical or HPLC grade and were purchased from Sigma−Aldrich, Alfa-Aesar, or ACROS Organics. Sodium methoxide solution (25 wt % in methanol) was purchased from Sigma−Aldrich. For anhydrous reactions, glassware was dried overnight in a 100−150 °C oven and purged with argon before use. Solvents were dried by stirring with activated 4 Å molecular sieves overnight under argon. Thin-layer chromatography (TLC) was performed using aluminum sheet TLC plates (0.25 mm)

https://doi.org/10.1021/acschembio.1c00063
ACS Chem. Biol. XXXX, XXX, XXX−XXX

precoated with Merck silica gel 60 F254, using ethyl acetate:/hexanes, toluene/acetone, water/methanol/ethyl acetate, or water/isopropanol/ethyl acetate as solvent systems (particular solvent ratios specified below), and visualized by a UV lamp and/or 10% sulfuric acid in water with charring using a heat gun. Flash chromatography was performed using Merck silica gel 60 with the same eluent systems as used for the corresponding TLC. The Amberlite IR120H$^+$ resin was washed with a copious amount of methanol before use.

All ^{19}F-, ^{13}C- and ^{1}H NMR data were collected on a Bruker Avance 400 MHz spectrometer at RT (100.6 and 376.5 MHz for ^{13}C and ^{19}F, respectively). ^{1}H NMR spectra were referenced to $CHCl_3$ at 7.27 ppm or HOD at 4.79 ppm, ^{13}C NMR spectra were referenced to $CDCl_3$ at 77.0 ppm, and ^{19}F NMR spectra were referenced to $CFCl_3$ at 0.00 ppm.[122] MALDI-TOF MS data were collected on a Bruker Autoflex instrument in reflectron mode over m/z 700−3500, using 6-Aza-2-thiothymine (ATT) as the matrix. ESCI MS was performed on a Waters LC-MS system including Waters 2695 HPLC and Waters ZQ mass spectrometer. HRMS data were obtained using either a Waters Xevo G2-S Q-TOF or Waters/Micromass LCT TOF mass spectrometer in positive-ion mode, via direct infusion through an electrospray ion source. HPAEC-PAD was performed on a Dionex ICS-5000 system equipped with an AS-AP autosampler and temperature-controlled sample tray, run in a sequential injection configuration using CHROMELEON 7 software, as described previously.[35,54,87]

Preparation of Laminaribiose (G3G) per-O-Acetate. Laminaribiose (G3G) was prepared by enzymatic hydrolysis of 3 g of the commercially available polysaccharide laminarin from *Laminaria digitate*, using *Bu*GH16, which yielded a mixture of glucose, G3G, and a small amount of a mixed-linkage trisaccharide, as described previously.[54] This mixture was acetylated by dissolving in pyridine (60 mL) and acetic anhydride (40 mL), followed by heating to 60 °C for 3 h. Following workup, the crude mixture was purified using column chromatography with toluene/acetone (6.5:1) as the eluent to yield 3.5 g of pure (per-OAc)G3G (R_f = 0.33). The characterization data were in accordance with literature values.[90]

Preparation of GG3G and GGG3G Mixed-Linkage Oligosaccharides and per-O-Acetates. Oat β-glucan powder (30 g, 70% purity; Garuda International, CA, USA) was suspended in 25 mM sodium citrate buffer, pH 6.5 (1 L), heated to 50 °C, and stirred for 20 min. 100 μL of 0.45 mM *Bo*GH16 was added to this suspension and the reaction was stirred overnight at 37 °C, following which the mixture was concentrated under reduced pressure. The resulting syrup was then freeze-dried under vacuum to yield a pale powder, confirmed by HPAEC-PAD chromatography to contain a mixture of trisaccharide Glcβ-(1,4)-Glcβ(1,3)-Glc (**GG3G**) and tetrasaccharide Glcβ(1,4)-Glcβ(1,4)-Glcβ(1,3)-Glc (**GGG3G**) as the only oligosaccharides (Figure S8 in the Supporting Information).[35]

20 g of this mixture was per-*O*-acetylated at 60 °C using pyridine (150 mL) and acetic anhydride (100 mL) with *N*,*N*-dimethylaminopyridine (0.5 g) as a catalyst. After 3 h, the reaction mixture was concentrated under reduced pressure to near dryness, and subsequently dissolved in 7 mL of dichloromethane (DCM) and loaded onto a silica flash column. The peracetylated trisaccharide and tetrasaccharide were separated using flash chromatography with isocratic toluene/acetone (6.5:1) as the solvent system ((per-OAc)GG3G: R_f 0.3, yield = 3 g, (per-OAc)GGG3G: R_f 0.25, yield = 1 g). The per-*O*-acetylated oligosaccharides were stored at RT and were subsequently deprotected under Zemplen conditions using catalytic NaOMe in MeOH/DCM (9:1) as a solvent, followed by stirring at 4 °C overnight), as needed. The characterization of the resulting deprotected oligosaccharides, as well as their corresponding peracetylated congeners, was in accordance with previous literature.[58,123,124]

Preparation of G3GGG Oligosaccharide and per-O-Acetate. **G3GGG** was prepared by scaling-up our previously described enzyme hydrolysis method,[87] with modifications. Thus, 5 g of oat β-glucan powder (70%) was suspended in 25 mM sodium citrate buffer, pH 6 (1 L). 100 μL of 600 μM *Vv*EG16 (ΔV152) was added and the reaction was stirred for 48 h at 37 °C. Upon concentration under reduced pressure and subsequent lyophilization, a pale powder was obtained. This powder was confirmed by HPAEC-PAD to contain a mixture of glucose, cellobiose, and Glcβ(1,3)-Glcβ(1,4)-Glcβ(1,4)-Glc (**G3GGG**) (Figure S9 in the Supporting Information). Isolation of the pure per-*O*-acetylated oligosaccharide (per-OAc)G3GGG was achieved using the acetylation and flash chromatography conditions as described in the previous section (yield = 700 mg). Zemplen deprotection (MeOH/DCM (9:1) containing catalytic NaOMe, followed by stirring at 4 °C overnight), yielded the pure deprotected oligosaccharide in near quantitative yield.

(per-OAc)G3GGG. R_f = 0.25 (toluene/acetone: 6.5:1). ^{1}H NMR ($CDCl_3$, 400 MHz; see Figure S10 in the Supporting Information): δ 6.21 (H1α, d, J_{H1-H2} = 3.69 Hz, 0.45 H), 5.62 (H1β, d, J_{H1-H2} = 8.39 Hz, 0.54 H), 5.38 (t, J = 9.78, 0.5H), 5.19 (dd, J = 9.27, 8.95, 0.5H), 5.08- 4.78 (m, 7H), 4.52−3.55 (m, 19H), 2.14−1.94 (s, CH_3). ^{13}C NMR: ($CDCl_3$, 100.6 MHz, Figure S11 in the Supporting Information): δ 168.56−170.69 (CO), 100.89, 100.73, 100.37 (C1^{II}, C1^{III}, C1^{IV}), 91.64 (C1β), 89.02 (C1α), 78.65, 76.33, 76.04, 75.8, 75.69, 73.65, 73.02, 72.92, 72.86, 72.83, 72.66, 72.6, 72.4, 72.26, 71.84, 71.76, 71.11, 70.85, 70.63, 69.53, 69.47, 68.01, 67.89, 62.37, 61.86, 61.70, 61.32, 20.95−20.44 ($COCH_3$); monoisotopic m/z calculated for $C_{52}H_{70}O_{35}Na^+$: 1277.35954; LC-MS found: 1277.6; ESI-HRMS found: 1277.3602

G3GGG. ^{1}H NMR ($CDCl_3$, 400 MHz, Figure S12 in the Supporting Information): δ 5.24 (H1α, d, J_{H1-H2} = 3.72 Hz 0.40H), 4.76 (H1^{II}, d, J_{H1-H2} = 7.95 Hz, 1H), 4.67 (H1β, d, J_{H1-H2} = 7.95 Hz, 0.63H), 4.55 (H1^{III}, H1^{IV}, d, d, J = 8.14 Hz, 7.95 Hz, 2H), 4.01−3.27 (m, 23 H); ^{13}C NMR (D_2O, 100.6 MHz, Figure S13 in the Supporting Information): δ 102.98, 102.76, 102.52 (C1^{II}, C1^{III}, C1^{IV}), 95.96 (C1β), 92.02 (C1α), 84.14, 78.83, 78.68, 78.59, 78.57, 76.19, 75.79, 75.74, 75.68, 75.01, 74.45, 74.26, 74.1, 73.63, 73.19, 73.15, 71.5, 71.43, 70.32, 69.78, 69.65, 68.19, 60.89, 60.76, 60.20, 60.08; Monoisotopic m/z calculated for $C_{24}H_{42}O_{21}Na^+$: 689.21163; LC-MS found: 689.2; ESI-HRMS found: 689.2115.

Synthesis of N-Bromoacetylglycosylamines. The new *N*-bromoacetylglycosylamines were obtained by adapting previously established methods (Scheme 2).[13,77] 150 mg of **GG3G**, **GGG3G**, or **G3GGG** was dissolved in 15 mL of 30% ammonium hydroxide, and ammonium bicarbonate (2 equiv) was added to the mixture. The mixture was then stirred overnight (20 h) at 42 °C, and thereafter concentrated under reduced pressure to a powder before lyophilization to yield the corresponding β-aminoglycoside as a pale amorphous solid. Because of their inherent acid lability, these crude compounds were used directly without isolation.

GG3G-β-NH$_2$ (1). ^{1}H NMR (D_2O, 400 MHz, Figure S14 in the Supporting Information): δ 4.73 (H1^{II}, d, J = 9.28 Hz, 1H), 4.51 (H1^{III}, d, J = 8.27 Hz, 1H), 4.13−3.29 (m, 18 H).

GGG3G-β-NH$_2$ (2). ^{1}H NMR (D_2O, 400 MHz, Figure S15 in the Supporting Information): δ 4.70 (H1^{II}, d, J = 9.15 Hz, 1H), 4.50 (H1^{III}, d, J = 8.60 Hz, 1H), 4.48 (H1^{IV}, d, J = 7.96 Hz, 1H), 4.10−3.15 (m, 24H).

G3GGG-β-NH$_2$ (3). ^{1}H NMR (D_2O, 400 MHz, Figure S16 in the Supporting Information): δ 4.74 (H1^{II}, d, 1H), 4.55 (H1^{III}, d, J = 7.85 Hz, 1H), 4.53 (H1^{IV}, d, J = 8.07 Hz, 1H), 4.13−3.18 (m, 24H).

Each β-aminoglycoside (150 mg) was subsequently dissolved in 7 mL of dry *N*,*N*-dimethylformamide (DMF) under an inert atmosphere and stirred for 10 min to form a pale-yellow suspension. Bromoacetic anhydride (1.5 equiv) was added to the reaction mixture as a solution in 0.5 mL dry DMF solution through a syringe. Thereafter, the solution turned into a homogeneous dark yellow color. The reaction was monitored via TLC. Generally, the reaction time was 1.5−2 h. The reaction mixture was concentrated in the presence of silica (7 g) and dry-loaded onto a flash column. The product was eluted using a water/isopropanol/ethyl acetate (1:3:6) solvent system. Fractions containing the product were pooled together, concentrated, and dried to a pale powder. The yields after purification were 100 mg (yield: 54%, purity estimated by ^{1}H NMR: >95%) for **1**, 44 mg (yield: 25%, purity estimated by ^{1}H NMR: >95%) for **2**, and 68 mg (yield: 39%, purity estimated by ^{1}H NMR: >95%) for **3**.

https://doi.org/10.1021/acschembio.1c00063
ACS Chem. Biol. XXXX, XXX, XXX−XXX

*GG3G-β-NHCOCH$_2$Br (**4**).* R_f = 0.25 (water/isopropanol/ethyl acetate 1:3:6); ^{1}H NMR (D_2O, 400 MHz, Figure S17 in the Supporting Information): δ 5.05 (H1β, d, J = 9.30 Hz, 1H), 4.84 (H1^{II}, d, J = 8.06 Hz, 1H), 4.57 (H1^{III}, d, J = 7.82 Hz, 1H), 4.03 (s, $COCH_2Br$, 2H), 3.98−3.37 (m, 18H); ^{13}C NMR: (D_2O, 100.6 MHz, Figure S18 in the Supporting Information): δ 171.31 (C═O), 102.77, 102.74, 84.92, 79.76, 78.79, 77.58, 76.73, 76.18, 75.69, 75.05, 74.34, 73.38, 71.65, 69.69, 67.97, 60.83, 60.26, 60.07, 28.16 (CH_2Br); monoisotopic m/z calculated for $C_{20}H_{34}BrNO_{16}Na^+$: 646.09587; LC-MS found: 646.1; ESI-HRMS found: 646.0948.

*GGG3G-β-NHCOCH$_2$Br (**5**).* R_f = 0.25 (water/isopropanol/ethyl acetate 1:3:6); ^{1}H NMR (D_2O, 400 MHz, Figure S19 in the Supporting Information): δ 5.03 (H1β, d, J = 9.31 Hz, 1H), 4.82 (H1^{II}, d, 1H), 4.54 (H1^{III}, H1^{IV}, d, d, J = 8.36 Hz, J = 8.42 Hz, 2H), 4.00 (s, $COCH_2Br$, 2H), 4.02−3.33 (m, 24H); ^{13}C NMR: (D_2O, 100.6 MHz, Figure S20 in the Supporting Information): δ 171.34 (C═O), 102.77, 102.5, 79.74, 78.61, 78.05, 76.72, 76.19, 75.69, 75.1, 75.05, 74.24, 73.35, 73.14, 71.75, 69.66, 60.78, 60.12, 59.95, 27.98 (CH_2Br); monoisotopic m/z calculated for $C_{26}H_{44}BrNO_{21}Na^+$: 808.14870; LC-MS found: 808.5; ESI-HRMS found: 808.1477.

*G3GGG-β-NHCOCH$_2$Br (**6**).* R_f = 0.25 (water/isopropanol/ethyl acetate 1:3:6); ^{1}H NMR (D_2O, 400 MHz, Figure S21 in the Supporting Information): δ 5.02 (H1β, d, J = 9.19 Hz, 1H), 4.76 (H1^{II}, d, 1H) 4.56 (H1^{III}, d, J = 8.19 Hz, 1H), 4.53 (H1^{IV}, d, J = 8.09 Hz, 1H), 4.00 (s, $COCH_2Br$, 2H), 3.95−3.31 (m, 24H); ^{13}C NMR: (D_2O, 100.6 MHz, Figure S22 in the Supporting Information): δ 171.32 (C═O), 102.99, 102.77, 102.50, 84.18, 79.75, 78.62, 78.08, 76.72, 76.19, 75.69, 75.04, 74.24, 73.24, 73.64, 73.36, 73.14, 71.75, 69.80, 69.67, 68.21, 60.97, 60.79, 60.13, 59.97, 28.04 (CH_2Br); monoisotopic m/z calculated for $C_{26}H_{44}BrNO_{21}Na^+$: 808.14870; LC-MS found: 808.1; ESI-HRMS found: 808.1483.

Synthesis of 2′,4′-Dinitrophenyl-2-deoxy-2-fluoro-β-glycosides. The synthesis of the new 2-deoxy-2-fluoro-2′,4′-dinitrophenyl β-glycosides proceeded through a five-step protocol starting from the corresponding per-*O*-acetylated oligosaccharides (Scheme 3). Thus, (per-OAc)G3G (1.2 g) and (per-OAc)GG3G (1 g) were individually dissolved in 30 mL of dichloromethane and converted to their respective α-glycosyl bromides **7** and **8**, as per previously established protocols,[58,90] using 33% hydrogen bromide in glacial acetic acid. The characterization data of compounds **7** (81% yield) and **8** (89% yield) were in accordance with literature values.[58,90]

The per-*O*-acetylated **G3G** glycal (**9**) and per-*O*-acetylated **GG3G** glycal (**10**) were synthesized by adapting previously established methods.[21,125] Thus, the corresponding glycosyl α-bromide (1000 mg **7** or 900 mg **8**) was dissolved in 30 mL of acetic acid and slowly added to a suspension of Zn (31 equiv), NaOAc (18.5 equiv), and $CuSO_4{\cdot}5H_2O$ (0.2 equiv) in 20 mL of water, which had been stirring for 5 min. The solution was stirred vigorously for 3 h at RT and subsequently filtered through Celite. The mixture was concentrated under reduced pressure to remove the solvent, redissolved in DCM (100 mL), and washed with $NaHCO_3$ (3×) and brine (1×). The DCM layer was concentrated, and the resulting syrup was purified using flash chromatography with isocratic ethyl acetate/hexanes (1:1) as the mobile phase (for **9**: R_f = 0.3, for **10**: R_f = 0.25). The evaporation of solvents under reduced pressure yielded **9** (150 mg, 19% yield) and **10** (160 mg, 21% yield) as white solids.

*(per-OAc)G3G Glycal (**9**).* ^{1}H NMR (Figure S23 in the Supporting Information, 400 MHz, $CDCl_3$): δ 6.39 (d, $J_{(H1-H2)}$ = 6.26 Hz, 1H, H1), 5.18−5.11 (m, 2H, H1^{II}, H1^{III}), 5.00 (t, J = 9.62 Hz, 1H), 4.88 (dd, J = 8.37 Hz, J = 9.20 Hz, 1H), 4.79 (t, J = 5.10 Hz, 1 H), 4.65 (d, J = 7.97 Hz, 1H), 4.33−4.00 (m, 6 H), 3.69−3.65 (m, 1H), 1.92−2.01 (6s, 18H, $COCH_3$). ^{13}C NMR (Figure S24 in the Supporting Information, 100.6 MHz, $CDCl_3$): δ 171.15−169.31 (6× CO), 145.30 (C1), 98.85 (C1^{II}), 97.38 (C2), 73.93, 72.93, 72.00, 71.37, 69.96, 68.37, 67.92, 61.90 (C6/C6^{II}), 61.56 (C6/C6^{II}), 21.06−20.62 (6× CH_3); monoisotopic m/z calculated for $C_{24}H_{32}O_{15}Na^+$: 583.16390; MALDI-TOF MS found: 583.1; ESI-HRMS found: 583.1636.

*(per-OAc)GG3G Glycal (**10**).* ^{1}H NMR (Figure S25 in the Supporting Information, 400 MHz, $CDCl_3$): δ 6.45 (d, $J_{(H1-H2)}$ = 6.26 Hz, 1 H, H1), 5.25−5.23 (m, 1H), 5.19−4.82 (m, 6H), 4.66 (d, J = 8.05 Hz, 1H), 4.58 (dd, J = 12.01 Hz, J = 1.83 Hz, 1H), 4.52 (d, J = 7.97 Hz, 1H), 4.39−4.33 (m, 3H), 4.13−4.03 (m, 4H), 3.78 (t, J = 9.47 Hz, 1H), 3.68−3.60 (m, 2H), 2.13−1.98 (9s, 27H, $COCH_3$). ^{13}C NMR (Figure S26 in the Supporting Information, 100.6 MHz, $CDCl_3$): δ 170.64−169.17 (9 × CO), 145.26 (C1), 100.92 (C1^{III}), 99.06(C1^{II}), 97.44 (C2), 76.43, 74.03, 73.07, 73.00, 72.68, 72.13, 71.73, 71.66, 70.05, 68.00, 67.90, 61.79 (C6/C6^{II}/C6^{III}), 61.74 (C6/C6^{II}/C6^{III}), 61.67 (C6/C6^{II}/C6^{III}), 20.99−20.67 (9 × CH_3); monoisotopic m/z calculated for $C_{36}H_{48}O_{23}Na^+$: 871.24841; MALDI-TOF MS found: 871.3; ESI-HRMS found: 871.2483.

Utilizing established synthetic protocols[21,97,98] with modifications (see the Results and Discussion section), the glycals **9** (150 mg) and **10** (160 mg) were converted into a diastereomeric mixture of the corresponding (per-*O*-acetylated)-1-hydroxy 2-deoxy-2-fluoro-glycosides by dissolution in a minimum amount of acetone and addition to a stirring suspension of Selectfluor (1.2 equiv) in 18 mL of acetone/water (5:1). The solution was stirred first at RT for 16 h, and then at 60 °C for 3 h. It was subsequently filtered over a Celite plug and concentrated under reduced pressure. The resulting syrup was redissolved in minimum DCM and loaded to a silica column for partial purification using flash chromatography, using isocratic ethyl acetate/hexanes (1.2:1) as the eluent (R_f = 0.25−3.00 for **11** and **12**). This reaction yielded a mixture of diastereomers of **11** (60 mg, 38% yield) and **12** (90 mg, 54% yield) respectively, because of the addition of 2-fluoro and 1-hydroxyl functional groups either equatorially or axially. These mixtures were characterized using ^{19}F NMR and high-resolution mass spectrometry and were used in the next step without further purification.

*(per-OAc)-1-Hydroxy-2-deoxy-2-fluoro-G3G (**11**).* ^{19}F NMR (Figure S27, 376.5 MHz, $CDCl_3$): δ −199.17 (ddd, $J_{(F2-H2)}$ = 50.96 Hz, $J_{(F2-H3)}$ = 14.47 Hz, $J_{(F2-H1)}$ = 1.55 Hz, 0.13F, *gluco* β-anomer), −200.60 (dd, $J_{(F2-H2)}$ = 49.39 Hz, $J_{(F2-H3)}$ = 12.66 Hz, 0.59F, *gluco* α-anomer), −205.68 (ddd, $J_{(F2-H2)}$ = 49.60 Hz, $J_{(F2-H3)}$ = 27.70 Hz, $J_{(F2-H1)}$ = 6.18 Hz, 1F, *manno* α-anomer); Monoisotopic m/z calculated for $C_{24}H_{33}O_{16}FNa^+$: 619.16504; MALDI-TOF MS found: 619.1; ESI-HRMS found: 619.1650.

*(per-OAc)-1-Hydroxy-2-deoxy-2-fluoro-GG3G (**12**).* ^{19}F NMR (Figure S28 in the Supporting Information, 376.5 MHz, $CDCl_3$): δ −198.84 (ddd, $J_{(F2-H2)}$ = 51.11 Hz, $J_{(F2-H3)}$ = 15.11 Hz, $J_{(F2-H1)}$ = 1.91 Hz, 0.06 F, *gluco* β-anomer), −200.40 (dd, $J_{(F2-H2)}$ = 49.51 Hz, $J_{(F2-H3)}$ = 12.63 Hz, 0.39 F, *gluco* α-anomer), −205.82 (ddd, $J_{(F2-H2)}$ = 49.33 Hz, $J_{(F2-H3)}$ = 27.53 Hz, $J_{(F2-H1)}$ = 6.70 Hz, 1 F, *manno* α-anomer); monoisotopic m/z calculated for $C_{36}H_{49}O_{24}FNa^+$: 907.24956; MALDI-TOF MS found: 907.1; ESI-HRMS found: 907.2496.

The synthesis of the per-*O*-acetylated 2′,4′-dinitrophenyl-2-deoxy-2-fluoro-β-glycosides **13** and **14** followed previously reported glycosylation methods,[21,75] with modifications. The diastereomeric mixtures comprising **11** (60 mg) or **12** (90 mg) were individually dissolved in 5 mL of dry DMF containing 4 Å activated molecular sieves and anhydrous DABCO (5 equiv). A solution of 2 equiv of 2,4-DNFB in 1 mL of dry DMF was added to the reaction mixture through an oven-dried steel needle. The reaction was stirred for 3.5 h, concentrated using a rotary evaporator, redissolved in DCM (100 mL), and washed with $NaHCO_3$(3×) and brine (1×). TLC analysis of the product mixtures using toluene/acetone (2.5:1) indicated 3 spots each when visualized under UV lamp (indicating the presence of aromatic group), as well as on charring after dipping in 10% sulfuric acid solution [R_f = 0.40 (A1), 0.47 (A2), 0.55 (A3) for the diastereomeric mixture from **11**, and R_f = 0.34 (B1), 0.38 (B2), 0.47 (B3) for the diastereomeric mixture from **12**]. The fractions corresponding to the spots at R_f = 0.47 (A2) and 0.38 (B2) were separated by column chromatography using isocratic elution with toluene/acetone (6.5:1) and identified to be the desired *gluco* β diastereomers **13** and **14**, respectively. The spots A1/B1 and A3/B3 were identified to be the *manno* α and *gluco* α-diastereomers, respectively (for ^{19}F NMR spectra and assignments of A1 and A3, see Figures S29 and S30, respectively, in the Supporting Information). The column fractions containing the desired product were pooled and

https://doi.org/10.1021/acschembio.1c00063
ACS Chem. Biol. XXXX, XXX, XXX−XXX

concentrated using rotary evaporation to yield pure **13** (24 mg, 33%) and **14** (26 mg, 24%).

*(per-OAc)-2′,4′-Dinitrophenyl-2-deoxy-2-fluoro-β-G3G (**13**).* ^{1}H NMR (Figure S31 in the Supporting Information, 400 MHz, $CDCl_3$): δ 8.78 (d, $J_{(H'3\text{-}H'5)}$ = 2.70 Hz, 1H, H′3), 8.44 (dd, $J_{(H'5\text{-}H'6)}$ = 9.16 Hz, $J_{(H'5\text{-}H'3)}$ = 2.70 Hz, 1H, H′5), 7.39 (d, $J_{(H'6\text{-}H'5)}$ = 9.16 Hz, 1H, H′6), 5.29 (dd, $J_{(H1\text{–}H2)}$ = 7.47 Hz, $J_{(H1\text{–}H3)}$ = 3.43 Hz, 1H, H1), 5.25−4.96 (m, 4H), 4.74 (d, $J_{(H1II\text{–}H2II)}$ = 7.86 Hz, 1H, $H1^{II}$), 4.69−4.64 (m, 1H), 4.34 (dd, *J* = 12.51 Hz, *J* = 4.23 Hz, 1H), 4.22 (d, *J* = 3.76 Hz, 2H), 4.14−4.07 (m, 2H), 3.94−3.89 (m, 1H), 3.72−3.68 (m, 1H), 2.10−2.01 (6s, 18H, $COCH_3$). ^{13}C NMR (Figure S32 in the Supporting Information, 100.6 MHz, $CDCl_3$): δ 170.46−169.05 (6 × CO), 153.39 (C′3), 142.43 (C′4), 140.38 (C′5), 128.56 (C′1), 121.72 (C′2), 118.39(C′6), 101.39 ($C1^{II}$), 98.59 ($J_{(C1\text{–}F2)}$ = 24.93 Hz, C1), 91.07 ($J_{(C2\text{–}F2)}$ = 190.19 Hz, C2), 79.47, ($J_{(C3\text{–}F2)}$ = 18.13 Hz, C3), 72.85, 72.56, 71.88, 71.33, 67.97 ($C4^{II}$), 67.37 ($J_{(C4\text{–}F2)}$ = 8.31 Hz, C4), 61.70 (C6, $C6^{II}$), 20.69−20.33 (6 × CH_3). ^{19}F NMR (Figure S33 in the Supporting Information, 376.5 MHz, $CDCl_3$): δ −198.81 (ddd, $J_{(F2\text{–}H2)}$ = 50.51 Hz, $J_{(F2\text{–}H3)}$ = 15.27 Hz, $J_{(F2\text{–}H1)}$ = 3.17 Hz, *gluco* β-anomer); Monoisotopic *m*/*z* calculated for $C_{30}H_{35}O_{20}N_2FNa^+$: 785.16650; MALDI-TOF MS found: 785.2; ESI-HRMS found: 785.1667.

*(per-OAc)-2′,4′-Dinitrophenyl-2-deoxy-2-fluoro-β-GG3G (**14**).* ^{1}H NMR (Figure S34 in the Supporting Information, 400 MHz, $CDCl_3$): δ 8.76 (d, $J_{(H'3\text{-}H'5)}$ = 2.38 Hz, 1H, H′3), 8.43 (d, $J_{(H'5\text{-}H'6)}$ = 9.16 Hz, $J_{(H'5\text{-}H'3)}$ = 2.38 Hz, 1H, H′5), 7.38 (d, $J_{(H'6\text{-}H'5)}$ = 9.16 Hz, 1H, H′6), 5.28 (dd, $J_{(H1\text{–}H2)}$ = 7.36 Hz, *J* = 3.97 Hz, 1H, H1), 5.23−5.00 (m, 5H), 4.91 (t, *J* = 8.07 Hz, 2H), 4.69 (d, $J_{(H1II\text{–}H2II)}$ = 7.68 Hz, 1H, $H1^{II}$), 4.53−3.59 (m, 12H), 2.13−1.98 (9s, 27 H, $COCH_3$). ^{13}C NMR (Figure S35 in the Supporting Information, 100.6 MHz, $CDCl_3$): δ 170.54−169.00 (9 × CO), 153.41 (C′3), 142.36 (C′4), 140.28 (C′5), 128.60 (C′1), 121.78 (C′2), 118.22 (C′6), 101.39 ($C1^{III}$), 100.59 ($C1^{II}$), 98.47 ($J_{(C1\text{–}F2)}$ = 25.15 Hz, C1), 91.01 ($J_{(C2\text{–}F2)}$ = 191.14 Hz, C2), 79.58 ($J_{(C3\text{–}F2)}$ = 18.11 Hz, C3), 75.96, 72.89, 72.83, 72.76, 72.16, 72.04, 71.63, 71.50, 67.72, 67.29 ($J_{(C4\text{–}F2)}$ = 7.04 Hz, C4), 61.80 ($J_{(C6\text{–}F2)}$ = 23.14 Hz, C6), 61.50 ($C6^{II}$, $C6^{III}$), 20.82−20.43 (9 × CH_3). ^{19}F NMR (Figure S36 in the Supporting Information, 376.5 MHz, $CDCl_3$): δ −198.32 (ddd, $J_{(F2\text{–}H2)}$ = 50.23 Hz, $J_{(F2\text{–}H3)}$ = 15.28 Hz, $J_{(F2\text{–}H1)}$ = 3.54 Hz, *gluco* β-anomer); Monoisotopic *m*/*z* calculated for $C_{42}H_{51}O_{28}N_2FNa^+$: 1073.25102; MALDI-TOF MS found: 1073.6; ESI-HRMS found: 1073.2513.

The deprotected 2′,4′-dinitrophenyl 2-deoxy-2-fluoro-β-glycosides **15** and **16** were obtained by Zemplen deprotection of **13** (24 mg) or **14** (26 mg), respectively, in 10 mL methanol/DCM (9:1) containing catalytic NaOMe. The solution was stirred at 4 °C for 16 h and monitored by TLC. Upon completion, the reaction was neutralized by adding 3 g of silica and concentrated to dryness under reduced pressure to yield a pale silica powder to which the product was adsorbed. This powder was dry loaded on a flash column and pure product was eluted using water/methanol/ethyl acetate (1:2:18) as the mobile phase. The fractions containing the product were pooled together and concentrated to give a syrup, which was redissolved in water and freeze-dried to give a white, fluffy powder **15** (5.1 mg, yield: 30%, purity estimated by ^{1}H NMR: 95%) and **16** (6.6 mg, yield: 40%, purity estimated by ^{1}H NMR: 95%).

*2′,4′-Dinitrophenyl-2-deoxy-2-fluoro-β-G3G [G3G(2F)-β-DNP, **15**].* ^{1}H NMR (Figure S37 in the Supporting Information, 400 MHz, D_2O): δ 8.93 (d, $J_{(H'3\text{-}H'5)}$ = 2.65 Hz, 1H, H′3), 8.57 (dd, $J_{(H'5\text{-}H'6)}$ = 9.31 Hz, $J_{(H'5\text{-}H'3)}$ = 2.65 Hz, 1H, H′5), 7.64 (d, $J_{(H'6\text{-}H'5)}$ = 9.31 Hz, 1H, H′6), 5.78 (dd, $J_{(H1\text{–}H2)}$ = 7.62 Hz, *J* = 2.90 Hz, 1H, H1), 4.74 (d, $J_{(H1II\text{–}H2II)}$ = 7.71 Hz, 1H, $H1^{II}$), 4.30−4.22 (m, 1H), 4.01−3.33 (m, 11H). ^{13}C NMR (Figure S38 in the Supporting Information, 100.6 MHz, D_2O): δ 154.08 (C′3), 141.97 (C′4), 139.22 (C′5), 130.04 (C′1), 122.40 (C′2), 118.10 (C′6), 102.66 ($C1^{II}$), 97.91 ($J_{(C1\text{–}F2)}$ = 23.14 Hz, C1), 91.39 ($J_{(C2\text{–}F2)}$ = 188.12 Hz, C2), 81.43 ($J_{(C3\text{–}F2)}$ = 17.10 Hz, C3), 76.49, 76.18, 75.72, 73.38 (C5), 69.79 ($C4^{II}$), 67.40 ($J_{(C4\text{–}F2)}$ = 7.92 Hz, C4), 60.91 ($C6^{II}$), 60.21 ($J_{(C6\text{–}F2)}$ = 20.12 Hz, C6). ^{19}F NMR (Figure S39 in the Supporting Information, 376.5 MHz, D_2O): δ −199.39 (ddd, $J_{(F2\text{–}H2)}$ = 50.61 Hz, $J_{(F2\text{–}H3)}$ = 15.05 Hz, $J_{(F2\text{–}H1)}$ = 2.39 Hz, *gluco* β-anomer); Monoisotopic *m*/*z* calculated for $C_{18}H_{23}O_{14}N_2FNa^+$: 533.10311; MALDI-TOF MS found: 533.1; ESI-HRMS found: 533.1018.

*2′,4′-Dinitrophenyl-2-deoxy-2-fluoro-β-GG3G [GG3G(2F)-β-DNP, **16**].* ^{1}H NMR (Figure S40 in the Supporting Information, 400 MHz, D_2O): δ 8.90 (d, $J_{(H'3\text{-}H'5)}$ = 2.50 Hz, 1H, H′3), 8.55 (dd, $J_{(H'5\text{-}H'6)}$ = 9.33 Hz, $J_{(H'5\text{-}H'3)}$ = 2.50 Hz, 1H, H′5), 7.62 (d, $J_{(H'6\text{-}H'5)}$ = 9.33 Hz, 1H, H′6), 5.76 (dd, $J_{(H1\text{–}H2)}$ = 7.36 Hz, *J* = 2.21 Hz, 1H, H1), 4.71 (d, $J_{(H1II\text{–}H2II)}$ = 7.40 Hz, 1H, $H1^{II}$), 4.51 (d, $J_{(H1III\text{–}H2III)}$ = 7.33 Hz, 1H, $H1^{III}$), 4.29−3.29 (m, 18H). ^{13}C NMR (Figure S41 in the Supporting Information, 100.6 MHz, D_2O): δ 153.86 (C′3), 141.72 (C′4), 138.94 (C′5), 129.86 (C′1), 122.19 (C′2), 117.89 (C′6), 102.54, ($C1^{III}$), 102.21 ($C1^{II}$), 97.65 ($J_{(C1\text{–}F2)}$ = 24.14 Hz, C1), 91.18 ($J_{(C2\text{–}F2)}$ = 188.12 Hz, C2), 81.11 ($J_{(C3\text{–}F2)}$ = 16.09 Hz, C3), 78.53, 76.24, 75.94, 75.44, 74.77, 74.05, 73.12, 72.94, 67.50 ($C4^{II}$/^{III}), 67.14 ($J_{(C4\text{–}F2)}$ = 8.05 Hz, C4), 60.54 ($C6^{II}$, $C6^{III}$), 60.03 ($J_{(C6\text{–}F2)}$ = 11.06 Hz, C6). ^{19}F NMR (Figure S42 in the Supporting Information, 376.5 MHz, D_2O): δ −199.24 (ddd, $J_{(F2\text{–}H2)}$ = 50.88 Hz, $J_{(F2\text{–}H3)}$ = 15.02 Hz, $J_{(F2\text{–}H1)}$ = 2.42 Hz, *gluco* β-anomer); Monoisotopic *m*/*z* calculated for $C_{24}H_{33}O_{19}N_2FNa^+$: 695.15593; MALDI-TOF MS found: 695.1; ESI-HRMS found: 695.1552.

Enzyme Substrates. The chromogenic substrate GG3G 2′-chloro-4′-nitrophenyl β-glycoside (GG3G-β-CNP) was purchased from Megazyme International (Ireland, product code O-CNPBG3). G3G 2′-chloro-4′-nitrophenyl β-glycoside (GG3G-β-CNP) was synthesized from α-laminaribiosyl bromide (7) by adapting a previously established protocol,[126] as follows.

To circumvent partial de-*O*-acetylation often observed with traditional phase-transfer conditions,[127] the sodium salt of 2-chloro-4-nitrophenol (NaCNP) was prepared first by the addition of NaOH (400 mg) to an aqueous solution (50 mL) of 2-chloro-4-nitrophenol (CNP, 1.74 g). The solution was stirred for 10 min and subsequently acetone (200 mL) was added to precipitate the salt. The precipitated salt was filtered, washed with acetone several times, and stored as a dry powder (1.92 g, 98%) at 4 °C until further needed. A solution of the sodium phenolate salt (1.5 g, 4.5 equiv) in water (3 mL) was added to a solution of α-laminaribiosyl bromide[58] (7,1.2 g) and benzyl tri-*n*-butylammonium chloride (536 mg, 1 equiv) in DCM (120 mL). The reaction mixture was stirred at RT for 48 h and monitored via TLC analysis. Subsequently, it was diluted with more DCM (120 mL), washed with water (2×), dried over $MgSO_4$, and concentrated *in vacuo*. The pure compound (1.1 g, 81%) was isolated via flash chromatography using ethyl acetate/hexanes (3:4) as eluent (R_f = 0.25). Zemplen deprotection was performed by dissolving 1.1 g of the per-*O*-acetate in MeOH/DCM (9:1) (30 mL) containing catalytic NaOMe, followed by stirring at 4 °C overnight. The reaction mixture was then neutralized with Amberlite IR120 hydrogen foam and purified by flash chromatography (water/methanol/ethyl acetate (1:2:9) to afford the pure product (394 mg, 57%).

(per-OAc)-2′-Chloro-4′-nitrophenyl β-laminaribioside. ^{1}H NMR (Figure S43 in the Supporting Information, 400 MHz, $CDCl_3$): δ 8.30 (d, $J_{(H'3\text{-}H'5)}$ = 2.63 Hz, 1H, H′3), 8.12 (dd, $J_{(H'\text{-}H'6)}$ = 9.05 Hz, $J_{(H'5\text{-}H'3)}$ = 2.63 Hz, 1H, H′5), 7.22 (d, $J_{(H'6\text{-}H'5)}$ = 9.05 Hz, 1H, H′6), 5.40 (d, $J_{(H1\text{–}H2)}$ = 8.18 Hz, 1H, H1), 5.19−4.90 (m, 5H), 4.65 (d, $J_{(H2\text{–}H1)}$ = 8.18 Hz, 1H, H2), 4.39 (dd, *J* = 12.31 Hz, *J* = 4.32 Hz, 1H), 4.25−4.00 (m, 4H), 3.93−3.88 (m, 1H), 3.72−3.68 (m, 1H), 2.18−2.00 (7s, 21H, $COCH_3$). ^{13}C NMR (Figure S44 in the Supporting Information, 100.6 MHz, $CDCl_3$): δ 170.60−168.79 (7 × CO), 157.45 (C′3), 143.38 (C′4), 126.31 (C′5), 125.15 (C′1), 123.66 (C′2), 116.77 (C′6), 101.08 ($C1^{II}$), 99.52 (C1), 78.34 (C3), 72.97, 72.73, 71.92, 71.18, 68.12 (C2), 62.07 (C6 or $C6^{II}$), 61.82 (C6 or $C6^{II}$), 21.01−20.49 (7 × CH_3); monoisotopic *m*/*z* calculated for $C_{32}H_{38}O_{20}NClNa^+$: 814.15735; MALDI-TOF MS found: 814.3; ESI-HRMS found: 814.1571.

2′-Chloro-4′-nitrophenyl β-laminaribioside (G3G-β-CNP). ^{1}H NMR (Figure S45 in the Supporting Information, 400 MHz, D_2O): δ 8.33 (d, $J_{(H'3\text{-}H'5)}$ = 2.75 Hz, 1H, H′3), 8.21 (dd, $J_{(H'5\text{-}H'6)}$ = 9.19 Hz, $J_{(H'5\text{-}H'3)}$ = 2.75 Hz, 1H, H′5), 7.46 (d, $J_{(H'6\text{-}H'5)}$ = 9.19 Hz, 1H, H′6), 5.27 (d, $J_{(H1\text{–}H2)}$ = 7.55 Hz, 1H, H1), 4.65 (d, $J_{(H1II\text{–}H2II)}$ = 7.93 Hz, 1H, $H1^{II}$), 3.95−3.32 (m, 12H). ^{13}C NMR (Figure S46 in the Supporting Information, 100.6 MHz, D_2O): δ 157.46 (C′3),142.67

https://doi.org/10.1021/acschembio.1c00063
ACS Chem. Biol. XXXX, XXX, XXX−XXX

(C′4), 126.39 (C′5), 124.49 (C′1), 123.56 (C′2), 115.82 (C′6), 102.98 (C1^{II}), 99.94 (C1), 83.77 (C3), 76.25, 76.21, 75.74, 73.65, 72.61, 69.80, 67.92, 60.91 (C6 or C6^{II}), 60.56 (C6 or C6^{II}); monoisotopic m/z calculated for $C_{18}H_{24}O_{13}NClNa^+$: 520.08339; MALDI-TOF MS found: 520.0; ESI-HRMS found: 520.0831.

Inhibition Kinetics. The determination of time-dependent enzyme inhibition kinetics was performed essentially as previously described.[13,21] Ultrapure water (18.2 MΩ cm^{-1}) was used for all kinetic experiments. 100 μL solutions of *Bo*GH16 (8.9 μM) were incubated with a range of concentrations of inhibitor (0.019−1.25 mM) at 37 °C in 50 mM sodium citrate buffer pH 6.5 (with 0.1 mg mL^{-1} bovine serum albumin to prevent nonspecific loss of activity). A control experiment was run in parallel, in which no inhibitor was added to the buffered enzyme/BSA solution. Periodically, 10 μL of this solution was withdrawn and diluted 1:100 in 50 mM sodium citrate pH 6.5 buffer, and 100 μL of the diluted incubate was added to 100 μL of the preincubated solution of chromogenic substrate GG3G-β-CNP in ultrapure water at 37 °C (0.2 mM final substrate concentration in the assay).

Residual activities were determined by measuring the rate of release of the chromophore 2-chloro-4-nitrophenolate (ε = 16.57 mM^{-1} cm^{-1}) over 1−2 min in a 1 cm quartz cuvette maintained at 37 °C at 405 nm in an Agilent Cary 60 UV−vis spectrophotometer with a Peltier temperature-controlled cell holder. The inhibition kinetics constants K_i and k_i were determined according to the Kitz−Wilson kinetics model (eq 1)[110] by fitting eqs 2 and 3 to the data by nonlinear regression using Origin Pro software, as previously described.[13,88]

$$E + I \overset{K_i}{\rightleftharpoons} E{\cdot}I \overset{k_i}{\rightarrow} E{\cdot}I \quad (1)$$

$$\nu = \nu_0 \, e^{-k_{app}t} \quad (2)$$

$$k_{app} = \frac{k_i[I]}{K_i + [I]} \quad (3)$$

The inhibition of the laminarinase *Bu*GH158 in the presence of compounds **15** and **16** was measured analogously, using the chromogenic substrate G3G-β-CNP to measure residual activity. The Michaelis−Menten kinetic parameters for G3G-β-CNP were first determined by directly fitting the Michaelis−Menten equation to data from duplicate assays over the concentration range of 0.078−7.5 mM in 50 mM sodium citrate buffer, pH 6, at 50 °C (optimum temperature of *Bu*GH158 activity[54]). Inhibition kinetics were performed in this same buffer and at the same temperature. Thus, 100 μL solution of 0.13 mM enzyme in buffer was incubated with the inhibitor (with 0.1 mg mL^{-1} bovine serum albumin added to prevent nonspecific loss of activity). The concentration range of each inhibitor was 10−0.31 mM. At various times up to 180 min, a 10 μL aliquot of this incubate was withdrawn and diluted 1:100 in the same buffer and 100 μL of this diluted enzyme−inhibitor incubate was mixed with 100 μL of a solution of G3G-β-CNP(0.25 mM after dilution). This solution was added to a 1 cm quartz cuvette that had been warmed to 50 °C and residual activity of the enzyme at that time interval was determined by measuring the rate of release of 2-chloro-4-nitrophenolate at 405 nm in an Agilent Cary 60 UV-vis spectrophotometer (ε = 15.8 mM^{-1} cm^{-1}). As above, inhibition kinetics parameters K_i and k_i were determined according to the Kitz−Wilson kinetics model.

Intact-Protein Mass Spectrometry. Intact-protein masses were determined on a Waters Xevo LC-ESI-MS Q-TOF with a NanoAcuity UPLC system using Masslynx 4.0 software, essentially as previously described.[128] For *N*-bromoacetylglycosylamine oligosaccharides, a 20 μL solution of *Bo*GH16 (3.27 μM in 50 mM pH 6.5 sodium citrate buffer) containing 2.5 mM inhibitor (765 eq. with respect to *Bo*GH16) was incubated for 3 h (for compounds **4** and **5**) or 7 h (for compound **6**) at 37 °C. For the 2-deoxy-2-fluoro-2′,4′-dinitrophenyl β-glycosides, a 20 μL solution of *Bu*GH158 (4.13 μM), *Bo*GH16 (2.60 μM), or *Bu*GH16 (4.24 μM) in 10 mM sodium citrate buffer, pH 6, containing 2.5 mM inhibitor was incubated at 50 °C for 2 h. The final equivalent molar values for each 2-deoxy-2-fluoro-2′,4′-dinitrophenyl β-glycoside inhibitor were 605 equiv (with respect to *Bu*GH158), 962 equiv (with respect to *Bo*GH16), and 590 equiv (with respect to *Bu*GH16). Negative controls omitting the inhibitors from the respective incubates were run in parallel.

Protein Crystallography. To reproduce previous crystallography,[35] crystals of unliganded recombinant *Bo*GH16 were obtained by first screening sitting drops in 96-well format at RT (setup using a Phoenix robot, Art Robbin). A hit observed in the JCSG+ screen (Qiagen) condition G7 was pursued for optimization by screening around this condition, varying the PEG concentration in one dimension and the buffer pH in the other (24-well format hanging drops, set up by hand). Large, orthorhombic crystals were readily reproduced by mixing 27.2 mg mL^{-1} protein solution one-to-one with reservoir solution comprised of 0.1 M succinic acid pH 7.2 and 15% (w/v) PEG3350. Crystals of the *Bo*GH16 E148A mutant were reproduced in identical concentration and conditions as the wild-type.

To obtain the *Bo*GH16:GGG3G-β-NHCOCH$_2$− complex structure, wild-type crystals were soaked for 1 h in mother liquor containing 2.5 mM of compound (**5**), after which time they were cryoprotected in mother liquor supplemented with 20% ethylene glycol. X-ray data from these crystals were collected at Advanced Photon Source beamline 23 ID-B. To obtain the *Bo*GH16:GG3G(2F) complex structure, crystals of *Bo*GH16E148A were soaked for 20 min in mother liquor containing 5 mM inhibitor, after which time they were cryoprotected in mother liquor supplemented with 25% ethylene glycol. X-ray data from these crystals were collected at Stanford Synchrotron Radiation Lightsource beamline BL12-2.

Datasets were indexed and integrated using XDS,[129] and scaled and merged using AIMLESS.[130] The structures were determined by molecular replacement using PHASER from the CCP4i2 software suite[131] with the original unliganded *Bo*GH16 structure (PDB ID: 5NBO)[35] as the search model. After density modification using PARROT,[132] iterative rounds of manual model building and refinement were performed in COOT[133] and REFMAC5,[134] respectively. The quality of the model was monitored using MOLPROBITY[135] and sugar conformations were validated using PRIVATEER.[136]

■ ASSOCIATED CONTENT

Supporting Information

The Supporting Information is available free of charge at https://pubs.acs.org/doi/10.1021/acschembio.1c00063.

Compound characterization checklist (XLS)

Crystallographic data tables for covalent enzyme complexes, supplementary protein mass spectrometry and kinetic data, HPLC analysis of oligosaccharides, and NMR spectra of synthetic intermediates and products (PDF)

Accession Codes

PDB accession 6VHO: Glycoside hydrolase family 16 endoglucanase from *Bacteroides ovatus* in complex with G4G4G3G-β-NHCOCH$_2$Br. PDB accession 7KR6: Glycoside hydrolase family 16 endoglucanase from *Bacteroides ovatus* in complex with G4G3G(2F)-β-DNP

■ AUTHOR INFORMATION

Corresponding Author

Harry Brumer − *Michael Smith Laboratories, University of British Columbia, Vancouver, British Columbia V6T 1Z4, Canada; Department of Chemistry, University of British Columbia, Vancouver, British Columbia V6T 1Z1, Canada; Department of Biochemistry and Molecular Biology, University of British Columbia, Vancouver, British Columbia V6T 1Z3, Canada;* orcid.org/0000-0002-0101-862X; Phone: (+1) 6048273738; Email: brumer@msl.ubc.ca; Fax: (+1) 6048222114

https://doi.org/10.1021/acschembio.1c00063
ACS Chem. Biol. XXXX, XXX, XXX−XXX

Authors

Namrata Jain − *Michael Smith Laboratories, University of British Columbia, Vancouver, British Columbia V6T 1Z4, Canada; Department of Chemistry, University of British Columbia, Vancouver, British Columbia V6T 1Z1, Canada*

Kazune Tamura − *Michael Smith Laboratories, University of British Columbia, Vancouver, British Columbia V6T 1Z4, Canada; Department of Biochemistry and Molecular Biology, University of British Columbia, Vancouver, British Columbia V6T 1Z3, Canada*

Guillaume Déjean − *Michael Smith Laboratories, University of British Columbia, Vancouver, British Columbia V6T 1Z4, Canada*

Filip Van Petegem − *Department of Biochemistry and Molecular Biology, University of British Columbia, Vancouver, British Columbia V6T 1Z3, Canada*

Complete contact information is available at: https://pubs.acs.org/10.1021/acschembio.1c00063

Author Contributions

N.J. performed the chemo-enzymatic synthesis of inhibitors, active site labeling, and inhibition kinetics experiments. K.T. performed recombinant protein production of *Bo*GH16, X-ray crystallography, analyzed enzyme structures, and provided advice on enzyme kinetics. G.D. produced *Bu*GH158 and *Bu*GH16 and provided advice on biochemistry. F.v.P. supervised crystallography. H.B. devised the overall study and supervised research. N.J., K.T., and H.B. cowrote the article.

Funding

Work in the Brumer Laboratory was generously supported by the Natural Sciences and Engineering Research Council of Canada (NSERC, Discovery Grant Nos. RGPIN 435223-13 and RGPIN-2018-03892), the Canadian Institutes of Health Research (CIHR, Operating Grant Nos. MOP-137134 and MOP-142472), as well as infrastructure support from the Canadian Foundation for Innovation (Project No. 30663) and the British Columbia Knowledge Development Fund. Work in the Van Petegem Lab was supported by the Canadian Institutes of Health Research (No. MOP-119404). K.T. was partially supported by a four-year doctoral fellowship from the University of British Columbia.

Notes

The authors declare no competing financial interest.

■ ACKNOWLEDGMENTS

We thank N. McGregor (Brumer Group, UBC) for producing *Vv*EG16(ΔV152) and J. Rogalski (UBC Proteomics Core Facility) for assistance with intact-protein MS analysis. H.B. gratefully acknowledges Waters Corporation for the provision of the LC-MS system used in this study.

■ ADDITIONAL NOTE

[a]Throughout, the widely used shorthand for mixed-linkage glucan oligosaccharides, is used, in which "3" indicates the position of the β(1,3) linkage between two glucosyl residues "G''. A β(1,3) linkage is otherwise indicated by default. Thus, G3G represents β-D-glucopyranosyl-(1,3)-D-glucopyranose (trivial name laminaribiose), GG3G represents β-D-glucopyranosyl-(1,4)-β-D-glucopyranosyl-(1,3)-D-glucopyranose, GGG3G represents β-D-glucopyranosyl-(1,4)-β-D-glucopyranosyl-(1,4)-β-D-glucopyranosyl-(1,3)-D-glucopyranose, and G3GGG β-D-glucopyranosyl-(1,3)-β-D-glucopyranosyl-(1,4)-β-D-glucopyranosyl-(1,4)-D-glucopyranose.

■ REFERENCES

(1) Lombard, V., Golaconda Ramulu, H., Drula, E., Coutinho, P. M., and Henrissat, B. (2014) The carbohydrate-active enzymes database (CAZy) in 2013. *Nucleic Acids Res. 42*, D490−D495.

(2) CAZypedia Consortium. (2018) Ten years of CAZypedia: A living encyclopedia of carbohydrate-active enzymes. *Glycobiology 28*, 3−8.

(3) Borges de Melo, E., da Silveira Gomes, A., and Carvalho, I. (2006) α- and β-Glucosidase inhibitors: chemical structure and biological activity. *Tetrahedron 62*, 10277−10302.

(4) Gloster, T. M., and Davies, G. J. (2010) Glycosidase inhibition: assessing mimicry of the transition state. *Org. Biomol. Chem. 8*, 305−320.

(5) Legler, G. (1990) Glycoside Hydrolases: Mechanistic Information from Studies with Reversible and Irreversible Inhibitors. *Adv. Carbohydr. Chem. Biochem. 48*, 319−384.

(6) Driguez, H. (2001) Thiooligosaccharides as tools for structural biology. *ChemBioChem 2*, 311−318.

(7) Kallemeijn, W. W., Witte, M. D., Wennekes, T., and Aerts, J. M. F. G. (2014) Mechanism-based inhibitors of glycosidases: Design and applications, In *Advances in Carbohydrate Chemistry and Biochemistry* (Horton, D., and Horton, D., Eds.), pp 297−338, Academic Press, New York.

(8) Rempel, B. P., and Withers, S. G. (2008) Covalent inhibitors of glycosidases and their applications in biochemistry and biology. *Glycobiology 18*, 570−586.

(9) Witte, M. D., Van Der Marel, G. A., Aerts, J. M. F. G., and Overkleeft, H. S. (2011) Irreversible inhibitors and activity-based probes as research tools in chemical glycobiology. *Org. Biomol. Chem. 9*, 5908−5926.

(10) Willems, L. I., Jiang, J., Li, K. Y., Witte, M. D., Kallemeijn, W. W., Beenakker, T. J. N., Schröder, S. P., Aerts, J. M. F. G., van der Marel, G. A., Codée, J. D. C., and Overkleeft, H. S. (2014) From covalent glycosidase inhibitors to activity-based glycosidase probes. *Chem. - Eur. J. 20*, 10864−10872.

(11) Xu, Y., Uddin, N., and Wagner, G. K. (2018) Covalent Probes for Carbohydrate-Active Enzymes: From Glycosidases to Glycosyltransferases. In *Methods in Enzymology* (Pyle, A. M., Christianson, D. W., Pyle, A. M., and Christianson, D. W., Eds.), pp 237−265, Cambridge.

(12) Wu, L., Armstrong, Z., Schröder, S. P., de Boer, C., Artola, M., Aerts, J. M. F. G., Overkleeft, H. S., and Davies, G. J. (2019) An overview of activity-based probes for glycosidases. *Curr. Opin. Chem. Biol. 53*, 25−36.

(13) Fenger, T. H., and Brumer, H. (2015) Synthesis and Analysis of Specific Covalent Inhibitors of endo-Xyloglucanases. *ChemBioChem 16*, 575−583.

(14) Jiang, J., Beenakker, T. J. M., Kallemeijn, W. W., van der Marel, G. A., van den Elst, H., Codée, J. D. C., Aerts, J. M. F. G., and Overkleeft, H. S. (2015) Comparing Cyclophellitol N-Alkyl and N-Acyl Cyclophellitol Aziridines as Activity-Based Glycosidase Probes. *Chem. - Eur. J. 21*, 10861−10869.

(15) Chakladar, S., Wang, Y., Clark, T., Cheng, L., Ko, S., Vocadlo, D. J., and Bennet, A. J. (2014) A mechanism-based inactivator of glycoside hydrolases involving formation of a transient non-classical carbocation. *Nat. Commun. 5*, 5590.

(16) Artola, M., Wu, L., Ferraz, M. J., Kuo, C. L., Raich, L., Breen, I. Z., Offen, W. A., Codée, J. D. C., Van Der Marel, G. A., Rovira, C., Aerts, J. M. F. G., Davies, G. J., and Overkleeft, H. S. (2017) 1,6-Cyclophellitol Cyclosulfates: A New Class of Irreversible Glycosidase Inhibitor. *ACS Cent. Sci. 3*, 784−793.

(17) Adamson, C., Pengelly, R. J., Shamsi Kazem Abadi, S., Chakladar, S., Draper, J., Britton, R., Gloster, T. M., and Bennet, A. J. (2016) Structural Snapshots for Mechanism-Based Inactivation of a Glycoside Hydrolase by Cyclopropyl Carbasugars. *Angew. Chem., Int. Ed. 55*, 14978−14982.

(18) Ren, W., Pengelly, R., Farren-Dai, M., Shamsi Kazem Abadi, S., Oehler, V., Akintola, O., Draper, J., Meanwell, M., Chakladar, S., Świderek, K., Moliner, V., Britton, R., Gloster, T. M., and Bennet, A. J. (2018) Revealing the mechanism for covalent inhibition of glycoside hydrolases by carbasugars at an atomic level. *Nat. Commun. 9*, 3243.
(19) Beenakker, T. J. M., Wander, D. P. A., Offen, W. A., Artola, M., Raich, L., Ferraz, M. J., Li, K. Y., Houben, J. H. P. M., Van Rijssel, E. R., Hansen, T., Van Der Marel, G. A., Codée, J. D. C., Aerts, J. M. F. G., Rovira, C., Davies, G. J., and Overkleeft, H. S. (2017) Carba-cyclophellitols Are Neutral Retaining-Glucosidase Inhibitors. *J. Am. Chem. Soc. 139*, 6534−6537.
(20) Hoj, P. B., Rodriguez, E. B., Iser, J. R., Stick, V. R., and Stone, B. A. (1991) Active site-directed inhibition by optically pure epoxyalkyl cellobiosides reveals differences in active site geometry of two 1,3−1,4-β-D-glucan 4-glucanohydrolases: The importance of epoxide stereochemistry for enzyme inactivation. *J. Biol. Chem. 266*, 11628−11631.
(21) Jain, N., Attia, M. A., Offen, W. A., Davies, G. J., and Brumer, H. (2018) Synthesis and application of a highly branched, mechanism-based 2-deoxy-2-fluoro-oligosaccharide inhibitor of endo-xyloglucanases. *Org. Biomol. Chem. 16*, 8732−8741.
(22) Kwan, D. H., Jin, Y., Jiang, J. B., Chen, H. M., Kotzler, M. P., Overkleeft, H. S., Davies, G. J., and Withers, S. G. (2016) Chemoenzymatic synthesis of 6-phospho-cyclophellitol as a novel probe of 6-phospho-beta-glucosidases. *FEBS Lett. 590*, 461−468.
(23) Stubbs, K. A. (2014) Activity-based proteomics probes for carbohydrate-processing enzymes: Current trends and future outlook. *Carbohydr. Res. 390*, 9−19.
(24) Armstrong, Z., Kuo, C. L., Lahav, D., Liu, B., Johnson, R., Beenakker, T. J. M., de Boer, C., Wong, C. S., van Rijssel, E. R., Debets, M. F., Florea, B. I., Hissink, C., Boot, R. G., Geurink, P. P., Ovaa, H., van der Stelt, M., van der Marel, G. M., Codee, J. D. C., Aerts, J., Wu, L., Overkleeft, H. S., and Davies, G. J. (2020) Manno-epi-cyclophellitols Enable Activity-Based Protein Profiling of Human alpha-Mannosidases and Discovery of New Golgi Mannosidase II Inhibitors. *J. Am. Chem. Soc. 142*, 13021−13029.
(25) McGregor, N. G. S., Artola, M., Nin-Hill, A., Linzel, D., Haon, M., Reijngoud, J., Ram, A., Rosso, M. N., van der Marel, G. A., Codee, J. D. C., van Wezel, G. P., Berrin, J. G., Rovira, C., Overkleeft, H. S., and Davies, G. J. (2020) Rational Design of Mechanism-Based Inhibitors and Activity-Based Probes for the Identification of Retaining alpha-L-Arabinofuranosidases. *J. Am. Chem. Soc. 142*, 4648−4662.
(26) Jariwala, P. B., Pellock, S. J., Goldfarb, D., Cloer, E. W., Artola, M., Simpson, J. B., Bhatt, A. P., Walton, W. G., Roberts, L. R., Major, M. B., Davies, G. J., Overkleeft, H. S., and Redinbo, M. R. (2020) Discovering the Microbial Enzymes Driving Drug Toxicity with Activity-Based Protein Profiling. *ACS Chem. Biol. 15*, 217−225.
(27) Burton, R. A., and Fincher, G. B. (2009) (1,3;1,4)-β-D-glucans in cell walls of the poaceae, lower plants, and fungi: A tale of two linkages. *Mol. Plant 2*, 873−882.
(28) Fincher, G. B. (2009) Exploring the evolution of (1,3;1,4)-β-D-glucans in plant cell walls: comparative genomics can help! *Curr. Opin. Plant Biol. 12*, 140−147.
(29) Salmeán, A. A., Duffieux, D., Harholt, J., Qin, F., Michel, G., Czjzek, M., Willats, W. G. T., and Hervé, C. (2017) Insoluble (1 → 3), (1 → 4)-β-D-glucan is a component of cell walls in brown algae (Phaeophyceae) and is masked by alginates in tissues. *Sci. Rep. 7*, 2880.
(30) Vogel, J. (2008) Unique aspects of the grass cell wall. *Curr. Opin. Plant Biol. 11*, 301−307.
(31) Popper, Z. A., Michel, G., Hervé, C., Domozych, D. S., Willats, W. G. T., Tuohy, M. G., Kloareg, B., and Stengel, D. B. (2011) Evolution and Diversity of Plant Cell Walls: From Algae to Flowering Plants. *Annu. Rev. Plant Biol. 62* (1), 567−590.
(32) Collins, H. M., Burton, R. A., Topping, D. L., Liao, M. L., Bacic, A., and Fincher, G. B. (2010) Variability in fine structures of noncellulosic cell wall polysaccharides from cereal grains: Potential importance in human health and nutrition. *Cereal Chem. 87*, 272−282.
(33) Wood, P. J. (2007) Cereal β-glucans in diet and health. *J. Cereal Sci. 46*, 230−238.
(34) El Khoury, D., Cuda, C., Luhovyy, B. L., and Anderson, G. H. (2012) Beta glucan: Health benefits in obesity and metabolic syndrome. *J. Nutr. Metab. 2012*, 1−28.
(35) Tamura, K., Hemsworth, G. R., Dejean, G., Rogers, T. E., Pudlo, N. A., Urs, K., Jain, N., Davies, G. J., Martens, E. C., and Brumer, H. (2017) Molecular Mechanism by which Prominent Human Gut Bacteroidetes Utilize Mixed-Linkage Beta- Glucans, Major Health-Promoting Cereal Polysaccharides. *Cell Rep. 21*, 417−430.
(36) Dong, J.-l., Yu, X., Dong, L.-e., and Shen, R.-l. (2017) In vitro fermentation of oat β-glucan and hydrolysates by fecal microbiota and selected probiotic strains. *J. Sci. Food Agric. 97*, 4198−4203.
(37) Hughes, S. A., Shewry, P. R., Gibson, G. R., McCleary, B. V., and Rastall, R. A. (2008) In vitro fermentation of oat and barley derived β-glucans by human faecal microbiota. *FEMS Microbiol. Ecol. 64*, 482−493.
(38) Jaskari, J., Kontula, P., Siitonen, A., Jousimies-Somer, H., Mattila-Sandholm, T., and Poutanen, K. (1998) Oat β-glucan and xylan hydrolysates as selective substrates for *Bifidobacterium* and *Lactobacillus* strains. *Appl. Microbiol. Biotechnol. 49*, 175−181.
(39) McNeil, N. I. (1984) The contribution of the large intestine to energy supplies in man. *Am. J. Clin. Nutr. 39*, 338−342.
(40) Stone, B. A. (2009) Chemistry of β-Glucans, In *Chemistry, Biochemistry, and Biology of 1−3 Beta Glucans and Related Polysaccharides* (Bacic, A., Fincher, G. B., and Stone, B. A., Eds.), pp 5−46, Academic Press, San Diego, CA.
(41) Fincher, G. B., and Stone, B. A. (2004) Chemistry of Nonstarch Polysaccharides. In *Encyclopedia of Grain Science* (Wrigley, C., Ed.), pp 206−223, Elsevier, Oxford.
(42) Hrmova, M., and Fincher, G. B. (2001) Structure-function relationships of β-D-glucan endo- and exohydrolases from higher plants. *Plant Mol. Biol. 47*, 73−91.
(43) Planas, A. (2000) Bacterial 1,3−1,4-β-glucanases: Structure, function and protein engineering. *Biochim. Biophys. Acta, Protein Struct. Mol. Enzymol. 1543*, 361−382.
(44) McGregor, N., Morar, M., Fenger, T. H., Stogios, P., Lenfant, N., Yin, V., Xu, X., Evdokimova, E., Cui, H., Henrissat, B., Savchenko, A., and Brumer, H. (2016) Structure-function analysis of a mixed-linkage β-glucanase/xyloglucanase from the key ruminal bacteroidetes *prevotella bryantii* B14. *J. Biol. Chem. 291*, 1175−1197.
(45) Viborg, A. H., Terrapon, N., Lombard, V., Michel, G., Czjzek, M., Henrissat, B., and Brumer, H. (2019) A subfamily roadmap of the evolutionarily diverse glycoside hydrolase family 16 (GH16). *J. Biol. Chem. 294*, 15973−15986.
(46) Aspeborg, H., Coutinho, P. M., Wang, Y., Brumer, H., and Henrissat, B. (2012) Evolution, substrate specificity and subfamily classification of glycoside hydrolase family 5 (GH5). *BMC Evol. Biol. 12*, 186.
(47) Bernardi, A. V., de Gouvêa, P. F., Gerolamo, L. E., Yonamine, D. K., de Lourdes de Lima Balico, L., Uyemura, S. A., and Dinamarco, T. M. (2018) Functional characterization of GH7 endo-1,4-β-glucanase from *Aspergillus fumigatus* and its potential industrial application. *Protein Expression Purif. 150*, 1−11.
(48) Yoshida, K., and Komae, K. (2006) A rice family 9 glycoside hydrolase isozyme with broad substrate specificity for hemicelluloses in type II cell walls. *Plant Cell Physiol. 47*, 1541−1554.
(49) Tamoi, M., Kurotaki, H., and Fukamizo, T. (2007) β-1,4-Glucanase-like protein from the cyanobacterium Synechocystis PCC6803 is a β-1,3−1,4-glucanase and functions in salt stress tolerance. *Biochem. J. 405*, 139−146.
(50) Foley, M. H., Déjean, G., Hemsworth, G. R., Davies, G. J., Brumer, H., and Koropatkin, N. M. (2019) A Cell-Surface GH9 Endo-Glucanase Coordinates with Surface Glycan-Binding Proteins to Mediate Xyloglucan Uptake in the Gut Symbiont Bacteroides ovatus. *J. Mol. Biol. 431*, 981−995.

https://doi.org/10.1021/acschembio.1c00063
ACS Chem. Biol. XXXX, XXX, XXX−XXX

(51) Bauer, M. W., Driskill, L. E., Callen, W., Snead, M. A., Mathur, E. J., and Kelly, R. M. (1999) An Endoglucanase, EglA, from the Hyperthermophilic Archaeon *Pyrococcus*. *J. Bacteriol. 181*, 284.
(52) Taylor, E. J., Goyal, A., Guerreiro, C. I. P. D., Prates, J. A. M., Money, V. A., Ferry, N., Morland, C., Planas, A., Macdonald, J. A., Stick, V. R., Gilbert, H. J., Fontes, C. M. G. A., and Davies, G. J. (2005) How family 26 glycoside hydrolases orchestrate catalysis on different polysaccharides: Structure and activity of a *Clostridium thermocellum* lichenase, *Ct*Lic26A. *J. Biol. Chem. 280*, 32761−32767.
(53) Sinnott, M. L. (1990) Catalytic Mechanisms of Enzymic Glycosyl Transfer. *Chem. Rev. 90*, 1171−1202.
(54) Déjean, G., Tamura, K., Cabrera, A., Jain, N., Pudlo, N. A., Pereira, G., Viborg, A. H., Van Petegem, F., Martens, E. C., and Brumer, H. (2020) Synergy between Cell Surface Glycosidases and Glycan-Binding Proteins Dictates the Utilization of Specific Beta-(1,3)-Glucans by Human Gut Bacteroides. *mBio 11*, 1−21.
(55) Chaari, F., and Chaabouni, S. E. (2019) Fungal β-1,3−1,4-glucanases: production, proprieties and biotechnological applications. *J. Sci. Food Agric. 99*, 2657−2664.
(56) Von Wettstein, D., Mikhaylenko, G., Froseth, J. A., and Kannangara, C. G. (2000) Improved barley broiler feed with transgenic malt containing heat-stable (1,3−1,4)-β-glucanase. *Proc. Natl. Acad. Sci. U. S. A. 97*, 13512−13517.
(57) Faijes, M., Pérez, X., Pérez, O., and Planas, A. (2003) Glycosynthase Activity of Bacillus licheniformis 1,3−1,4-β-Glucanase Mutants: Specificity, Kinetics, and Mechanism. *Biochemistry 42*, 13304−13318.
(58) Malet, C., Vallés, J., Bou, J., and Planas, A. (1996) A specific chromophoric substrate for activity assays of 1,3−1,4-β-D-glucan 4-glucanohydrolases. *J. Biotechnol. 48*, 209−219.
(59) Planas, A., Abel, M., Millet, O., Palasi, J., Pallares, C., and Viladot, J.-L. (1998) Synthesis of aryl 3-O-β-cellobiosyl-β-d-glucopyranosides for reactivity studies of 1,3- 1,4- β-glucanases. *Carbohydr. Res. 310*, 53−64.
(60) Moreau, V., Viladot, J. L., Samain, E., Planas, A., and Driguez, H. (1996) Design and chemoenzymatic synthesis of thiooligosaccharide inhibitors of 1,3:1,4-β-D-glucanases. *Bioorg. Med. Chem. 4*, 1849−1855.
(61) Money, V. A., Cartmell, A., Guerreiro, C. I. P. D., Ducros, V. M.-A., Fontes, C. M. G. A., Gilbert, H. J., and Davies, G. J. (2008) Probing the β-1,3:1,4 glucanase, CtLic26A, with a thio-oligosaccharide and enzyme variants. *Org. Biomol. Chem. 6*, 851−853.
(62) Hoj, P. B., Condron, R., Traeger, J. C., McAuliffe, J. C., and Stone, B. A. (1992) Identification of glutamic acid 105 at the active site of *Bacillus amyloliquefaciens* 1,3−1,4-β-D-glucan 4-glucanohydrolase using epoxide-based inhibitors. *J. Biol. Chem. 267*, 25059−25066.
(63) Hoj, P. B., Rodriguez, E. B., Stick, V. R., and Stone, B. A. (1989) Differences in active site structure in a family of β-glucan endohydrolases deduced from the kinetics of inactivation by epoxyalkyl β-oligoglucosides. *J. Biol. Chem. 264*, 4939−4947.
(64) Keitel, T., Simon, O., Borriss, R., and Heinemann, U. (1993) Molecular and active-site structure of a *Bacillus* 1,3−1,4-β-glucanase. *Proc. Natl. Acad. Sci. U. S. A. 90*, 5287−5291.
(65) Withers, S. G., Street, I. P., Bird, P., and Dolphin, D. H. (1987) 2-Deoxy-2-fluoroglucosides: A Novel Class of Mechanism-Based Glucosidase Inhibitors. *J. Am. Chem. Soc. 109*, 7530−7531.
(66) Yariv, J., Wilson, K. J., Hildesheim, J., and Blumberg, S. (1971) Labelling of the Active Site of β-galactosidase by N-bromoacetyl β-D-galactopyranosylamine. *FEBS Lett. 15*, 24−26.
(67) Withers, S. G., Rupitz, K., and Street, I. P. (1988) 2-Deoxy-2-fluoro-D-glycosyl fluorides. A new class of specific mechanism-based glycosidase inhibitors. *J. Biol. Chem. 263*, 7929−7932.
(68) Street, I. P., Kempton, J. B., and Withers, S. G. (1992) Inactivation of a β-glucosidase through the accumulation of a stable 2-deoxy-2-fluoro-α-D-glucopyranosyl-enzyme intermediate: A detailed investigation. *Biochemistry 31*, 9970−9978.
(69) Blanchard, J. E., and Withers, S. G. (2001) Rapid screening of the aglycone specificity of glycosidases: Applications to enzymatic synthesis of oligosaccharides. *Chem. Biol. 8*, 627−633.
(70) Miao, S., Ziser, L., Aebersold, R., and Withers, S. G. (1994) Identification of Glutamic Acid 78 as the Active Site Nucleophile in *Bacillus subtilis* Xylanase Using Electrospray Tandem Mass Spectrometry. *Biochemistry 33*, 7027−7032.
(71) Withers, S. G., Warren, A. J., Street, I. P., Rupitz, K., Kempton, J. B., and Aebersold, R. (1990) Unequivocal Demonstration of the Involvement of a Glutamate Residue as a Nucleophile in the Mechanism of a "Retaining" Glycosidase. *J. Am. Chem. Soc. 112*, 5887−5889.
(72) Gebler, J. C., Aebersold, R., and Withers, S. G. (1992) Glu-537, not Glu-461, is the nucleophile in the active site of (lac Z) β-galactosidase from *Escherichia coli*. *J. Biol. Chem. 267*, 11126−11130.
(73) Vocadlo, D. J., Davies, G. J., Laine, R., and Withers, S. G. (2001) Catalysis by hen egg-white lysozyme proceeds via a covalent intermediate. *Nature 412*, 835−838.
(74) Hart, D. O., He, S. M., Chany, C. J., Withers, S. G., Sims, P. F. G., Sinnott, M. L., and Brumer, H. (2000) Identification of Asp-130 as the catalytic nucleophile in the main alpha-galactosidase from *Phanerochaete chrysosporium*, a family 27 glycosyl hydrolase. *Biochemistry 39*, 9826−9836.
(75) McCarter, J. D., Adam, M. J., Braun, C., Namchuk, M., Tull, D., and Withers, S. G. (1993) Syntheses of 2-deoxy-2-fluoro mono- and oligo-saccharide glycosides from glycals and evaluation as glycosidase inhibitors. *Carbohydr. Res. 249*, 77−90.
(76) Tull, D., Burgoyne, D. L., Chow, D. T., Withers, S. G., and Aebersold, R. (1996) A Mass Spectrometry-Based Approach for Probing Enzyme Active Sites: Identification of Glu 127 in *Cellulomonas fimi* Exoglycanase as the Residue Modified by N-Bromoacetyl Cellobiosylamine. *Anal. Biochem. 234*, 119−125.
(77) Black, T. S., Kiss, L., Tull, D., and Withers, S. G. (1993) N-Bromoacetyl-glycopyranosylamines as affinity labels for a β-glucosidase and a cellulase. *Carbohydr. Res. 250*, 195−202.
(78) Fekete, C. A., and Kiss, L. (2013) A new approach in the active site investigation of an inverting β-D-xylosidase from *Thermobifida fusca* TM51. *Protein J. 32*, 97−105.
(79) Jäger, S., and Kiss, L. (2005) Investigation of the active site of the extracellular β-D-glucosidase from *Aspergillus carbonarius*. *World J. Microbiol. Biotechnol. 21*, 337−343.
(80) Keresztessy, Z., Kiss, L., and Hughes, M. A. (1994) Investigation of the active site of the cyanogenic β-D-glucosidase (linamarase) from *Manihot esculenta* Crantz (Cassava). II. Identification of Glu-198 as an active site carboxylate group with acid catalytic function. *Arch. Biochem. Biophys. 315*, 323−330.
(81) Kiss, T., Erdei, A., and Kiss, L. (2002) Investigation of the active site of the extracellular β-D-xylosidase from *Aspergillus carbonarius*. *Arch. Biochem. Biophys. 399*, 188−194.
(82) Vocadlo, D. J., Wicki, J., Rupitz, K., and Withers, S. G. (2002) A case for reverse protonation: Identification of Glu160 as an acid/base catalyst in *Thermoanaerobacterium saccharolyticum* β-xylosidase and detailed kinetic analysis of a site-directed mutant. *Biochemistry 41*, 9736−9746.
(83) Chir, J., Withers, S., Wan, C.-F., and Li, Y.-K. (2002) Identification of the two essential groups in the family 3 β-glucosidase from *Flavobacterium meningosepticum* by labelling and tandem mass spectrometric analysis. *Biochem. J. 365*, 857−863.
(84) Legler, G., Sinnott, M. L., and Withers, S. G. (1980) Catalysis by β-Glucosidase A3 of *Aspergillus wentii*. *J. Chem. Soc., Perkin Trans. 2*, 1376−1383.
(85) Viratelle, M., Yon, J. M., and Yariv, J. (1977) The inactivation of β-galactosidase by N-bromoacetyl-β-D-glucosylamine. *FEBS Lett. 79*, 109−112.
(86) Naider, F., Bohak, Z., and Yariv, J. (1972) Reversible alkylation of a methionyl residue near the active site of β-galactosidase. *Biochemistry 11*, 3202−3208.
(87) McGregor, N., Yin, V., Tung, C. C., Van Petegem, F., and Brumer, H. (2017) Crystallographic insight into the evolutionary origins of xyloglucan endotransglycosylases and endohydrolases. *Plant J. 89*, 651−670.

https://doi.org/10.1021/acschembio.1c00063
ACS Chem. Biol. XXXX, XXX, XXX−XXX

(88) Attia, M. A., Nelson, C. E., Offen, W. A., Jain, N., Davies, G. J., Gardner, J. G., and Brumer, H. (2018) In vitro and in vivo characterization of three *Cellvibrio japonicus* glycoside hydrolase family 5 members reveals potent xyloglucan backbone-cleaving functions. *Biotechnol. Biofuels 11*, 45−61.
(89) Xue, J., Guo, M., Gu, G., and Guo, Z. (2012) A Facile Synthesis of Nγ-Glycosyl Asparagine Conjugates and Short N-Linked Glycopeptides. *J. Carbohydr. Chem. 31*, 105−113.
(90) Marca, E., Valero-Gonzalez, J., Delso, I., Tejero, T., Hurtado-Guerrero, R., and Merino, P. (2013) Synthesis of O- and C-glycosides derived from β-(1,3)-D-glucans. *Carbohydr. Res. 382*, 9−18.
(91) Adam, M. J., Pate, B. D., Nesser, J. R., and Hall, L. D. (1983) A rapid, stereoselective synthesis of fluorinated carbohydrates: Addition of acetyl hypofluorite to vinyl ether derivatives of sugars. *Carbohydr. Res. 124*, 215−224.
(92) Adamson, J., Foster, A.B., Hall, L.D., Johnson, R.N., and Heese, R.H. (1970) Fluorinated Carbohydrates: 2-deoxy-2-fluoro-D-glucose and 2-deoxy-2-fluoro-D-mannose. *Carbohydr. Res. 15*, 351−359.
(93) Korytnyk, W., Valentekovic-Horvath, S., and Petrie, C. R. (1982) A convenient synthesis of 1,2-difluoro-1, 2-dideoxyhexoses using xenon fluoride. *Tetrahedron 38*, 2547−2550.
(94) Ido, T., Wan, C. N., Fowler, J. S., and Wolf, A. P. (1977) Fluorination with F2. A Convenient Synthesis of 2-Deoxy-2-fluoro-D-glucose. *J. Org. Chem. 42*, 2341−2342.
(95) Abdul-Ghani, M., Banks, E. R., Besheesh, M. K., Sharif, I., and Syvret, R. G. (1995) N-Halogeno compounds. Part 14. "Transfer fluorination" of quinuclidine using F-TEDA-BFc (Selectfluor reagent): laboratory synthesis of N-fluoroquinuclidinium salts not requiring the use of elemental fluorine. *J. Fluorine Chem. 73*, 255−257.
(96) Burkart, M. D., Zhang, Z., Hung, S. C., and Wong, C. H. (1997) A new method for the synthesis of fluoro-carbohydrates and glycosides using selectfluor. *J. Am. Chem. Soc. 119*, 11743−11746.
(97) Vincent, S. P., Burkart, M. D., Tsai, C. Y., Zhang, Z., and Wong, C. H. (1999) Electrophilic fluorination-nucleophilic addition reaction mediated by Selectfluor: Mechanistic studies and new applications. *J. Org. Chem. 64*, 5264−5279.
(98) Albert, M., dax, K., and Ortner, J. (1998) A novel direct route to 2-deoxy-2-fluoro-aldoses and their corresponding derivatives. *Tetrahedron 54*, 4839−4848.
(99) Benito, D., Matheu, M. I., Morère, A., Díaz, Y., and Castillón, S. (2008) Towards the preparation of 2″-deoxy-2″-fluoro-adenophostin A. Study of the glycosylation reaction. *Tetrahedron 64*, 10906−10911.
(100) Dohi, H., Périon, R., Durka, M., Bosco, M., Roué, Y., Moreau, F., Grizot, S., Ducruix, A., Escaich, S., and Vincent, S. P. (2008) Stereoselective glycal fluorophosphorylation: Synthesis of ADP-2-fluoroheptose, an inhibitor of the LPS Biosynthesis. *Chem. - Eur. J. 14*, 9530−9539.
(101) Ortner, J., Albert, M., Weber, H., and Dax, K. (1999) Studies on the Reaction of D-Glucal and its Derivatives with 1-Chloromethyl-4-Fluoro-1,4-Diazoniabicyclo[2.2.2]Octane Salts. *J. Carbohydr. Chem. 18*, 297−316.
(102) Vocadlo, D. J., and Withers, S. G. (2005) The chemical synthesis of 2-deoxy-2-fluorodisaccharide probes of the hen egg white lysozyme mechanism. *Carbohydr. Res. 340*, 379−388.
(103) Wolf, S., Berrio, R. M., and Meier, C. (2011) Synthesis of nonnatural nucleoside diphosphate sugars. *Eur. J. Org. Chem. 2011*, 6304−6313.
(104) Williams, S. J., Hekmat, O., and Withers, S. G. (2006) Synthesis and testing of mechanism-based protein-profiling probes for retaining endo-glycosidases. *ChemBioChem 7*, 116−124.
(105) Goddard-Borger, E. D., Fiege, B., Kwan, E. M., and Withers, S. G. (2011) Glycosynthase-Mediated Assembly of Xylanase Substrates and Inhibitors. *ChemBioChem 12*, 1703−1711.
(106) Sakai, K., Nakahara, Y., and Ogawa, T. (1990) Total synthesis of nonasaccharide repeating unit of plant-cell wall xyloglucan—an endogenous hormone which regulates cell-growth. *Tetrahedron Lett. 31*, 3035−3038.
(107) Dallabernardina, P., Schuhmacher, F., Seeberger, P. H., and Pfrengle, F. (2016) Automated glycan assembly of xyloglucan oligosaccharides. *Org. Biomol. Chem. 14*, 309−313.
(108) Dax, K., Albert, M., Ortner, J., and Paul, B. J. (2000) Synthesis of deoxyfluoro sugars from carbohydrate precursors. *Carbohydr. Res. 327*, 47−86.
(109) Davies, G. J., Wilson, K. S., and Henrissat, B. (1997) Nomenclature for sugar-binding subsites in glycosyl hydrolases. *Biochem. J. 321*, 557−559.
(110) Kitz, R., and Wilson, I. B. (1962) Esters of methanesulfonic acid as irreversible inhibitors of acetylcholinesterase. *J. Biol. Chem. 237*, 3245−3249.
(111) Mackenzie, L. F., Sulzenbacher, G., Divne, C., Jones, T. A., Woldike, H. F., Schulein, M., Withers, S. G., and Davies, G. J. (1998) Crystal structure of the family 7 endoglucanase I (Cel7B) from *Humicola insolens* at 2.2 Å resolution and identification of the catalytic nucleophile by trapping of the covalent glycosyl-enzyme intermediate. *Biochem. J. 335*, 409−416.
(112) Wang, Q., Tull, D., Meinke, A., Gilkes, N. R., Warren, R. A. J., Aebersold, R., and Withers, S. G. (1993) Glu280 is the nucleophile in the active site of *Clostridium thermocellum* CelC, a family A endo-β-1,4-glucanase. *J. Biol. Chem. 268*, 14096−14102.
(113) Ziser, L., Setyawati, I., and Withers, S. G. (1995) Syntheses and testing of substrates and mechanism-based inactivators for xylanases. *Carbohydr. Res. 274*, 137−153.
(114) McCarter, J. D., Adam, M. J., and Withers, S. G. (1992) Binding Energy and Catalysis. Fluorinated and deoxygenated glycosides as mechanistic probes of *Escherichia coli* (lacZ) β-galactosidase. *Biochem. J. 286*, 721−727.
(115) Shaikh, F. A., Müllegger, J., He, S., and Withers, S. G. (2007) Identification of the catalytic nucleophile in Family 42 β-galactosidases by intermediate trapping and peptide mapping: YesZ from *Bacillus subtilis*. *FEBS Lett. 581*, 2441−2446.
(116) Namchuk, M. N., and Withers, S. G. (1995) Mechanism of *Agrobacterium* β-Glucosidase: Kinetic Analysis of the Role of Noncovalent Enzyme/Substrate Interactions. *Biochemistry 34*, 16194−16202.
(117) Ly, H. D., and Withers, S. G. (1999) Mutagenesis of glycosidases. *Annu. Rev. Biochem. 68*, 487−522.
(118) Armstrong, Z., Liu, F., Chen, H. M., Hallam, S. J., and Withers, S. G. (2019) Systematic Screening of Synthetic Gene-Encoded Enzymes for Synthesis of Modified Glycosides. *ACS Catal. 9*, 3219−3227.
(119) Halford, B. (2020) Covalent drugs go from fringe field to fashionable endeavor. *Chem. Eng. News 98*, 28−33.
(120) Namchuk, M. N., McCarter, J. D., Becalski, A., Andrews, T., and Withers, S. G. (2000) The role of sugar substituents in glycoside hydrolysis. *J. Am. Chem. Soc. 122*, 1270−1277.
(121) Artimo, P., Jonnalagedda, M., Arnold, K., Baratin, D., Csardi, G., de Castro, E., Duvaud, S., Flegel, V., Fortier, A., Gasteiger, E., Grosdidier, A., Hernandez, C., Ioannidis, V., Kuznetsov, D., Liechti, R., Moretti, S., Mostaguir, K., Redaschi, N., Rossier, G., Xenarios, I., and Stockinger, H. (2012) ExPASy: SIB bioinformatics resource portal. *Nucleic Acids Res. 40*, W597−W603.
(122) Gottlieb, H. E., Kotlyar, V., and Nudelman, A. (1997) NMR chemical shifts of common laboratory solvents as trace impurities. *J. Org. Chem. 62*, 7512−7515.
(123) Abel, M., Segade, A., and Planas, A. (2009) Synthesis of an aryl 2-deoxy-β-glycosyl tetrasaccharide to probe retaining endo-glycosidase mechanism. *Tetrahedron: Asymmetry 20*, 847−850.
(124) Malet, C., Jimenez-Barbero, J., Bernabe, M., Brosa, C., and Planas, A. (1993) Stereochemical course and structure of the products of the enzymic action of endo-1,3−1-4-β-D-glucan 4-glucanohydrolase from *Bacillus licheniformis*. *Biochem. J. 296*, 753−758.
(125) Xu, X., Tan, Q., and Hayashi, M. (2008) Versatile and mild synthesis of Di- and trisaccharidic 2-enopyranosyl cyanides by cyanation of per-O-acetylglycals with trimethylsilyl cyanide catalyzed by palladium(II) acetate. *Synthesis 2008*, 770−776.

https://doi.org/10.1021/acschembio.1c00063
ACS Chem. Biol. XXXX, XXX, XXX−XXX

(126) Ibatullin, F. M., Baumann, M. J., Greffe, L., and Brumer, H. (2008) Kinetic Analyses of Retaining endo-(Xylo)glucanases from Plant and Microbial Sources Using New Chromogenic Xylogluco-Oligosaccharide Aryl Glycosides. *Biochemistry 47*, 7762−7769.
(127) Kleine, H. P., Weinberg, V. D., Kaufman, R. J., and Sidhu, R. S. (1985) Phase-transfer-catalyzed synthesis of 2,3,4,6-tetra-O-acetyl-β-d-galactopyranosides. *Carbohydr. Res. 142*, 333−337.
(128) Sundqvist, G., Stenvall, M., Berglund, H., Ottosson, J., and Brumer, H. (2007) A general, robust method for the quality control of intact proteins using LC-ESI-MS. *J. Chromatogr. B: Anal. Technol. Biomed. Life Sci. 852*, 188−194.
(129) Kabsch, W. (2010) XDS. *Acta Crystallogr., Sect. D: Biol. Crystallogr. 66*, 125−132.
(130) Evans, P. R., and Murshudov, G. N. (2013) How good are my data and what is the resolution? *Acta Crystallogr., Sect. D: Biol. Crystallogr. 69*, 1204−1214.
(131) McCoy, A. J., Grosse-Kunstleve, R. W., Adams, P. D., Winn, M. D., Storoni, L. C., and Read, R. J. (2007) Phaser crystallographic software. *J. Appl. Crystallogr. 40*, 658−674.
(132) Cowtan, K. (2010) Recent developments in classical density modification. *Acta Crystallogr., Sect. D: Biol. Crystallogr. 66*, 470−478.
(133) Emsley, P., and Cowtan, K. (2004) Coot: Model-building tools for molecular graphics. *Acta Crystallogr., Sect. D: Biol. Crystallogr. 60*, 2126−2132.
(134) Murshudov, G. N., Skubák, P., Lebedev, A. A., Pannu, N. S., Steiner, R. A., Nicholls, R. A., Winn, M. D., Long, F., and Vagin, A. A. (2011) REFMAC5 for the refinement of macromolecular crystal structures. *Acta Crystallogr., Sect. D: Biol. Crystallogr. 67*, 355−367.
(135) Davis, I. W., Leaver-Fay, A., Chen, V. B., Block, J. N., Kapral, G. J., Wang, X., Murray, L. W., Arendall, W. B., Snoeyink, J., Richardson, J. S., and Richardson, D. C. (2007) MolProbity: All-atom contacts and structure validation for proteins and nucleic acids. *Nucleic Acids Res. 35*, W375−W383.
(136) Agirre, J., Iglesias-Fernández, J., Rovira, C., Davies, G. J., Wilson, K. S., and Cowtan, K. D. (2015) Privateer: Software for the conformational validation of carbohydrate structures. *Nat. Struct. Mol. Biol. 22*, 833−834.
(137) Geoghegan, K. F., Dixon, H. B. F., Rosner, P. J., Hoth, L. R., Lanzetti, A. J., Borzilleri, K. A., Marr, E. S., Pezzullo, L. H., Martin, L. B., LeMotte, P. K., McColl, A. S., Kamath, A. V., and Stroh, J. G. (1999) Spontaneous alpha-N-6-phosphogluconoylation of a "His tag" in Escherichia coli: The cause of extra mass of 258 or 178 Da in fusion proteins. *Anal. Biochem. 267*, 169−184.

https://doi.org/10.1021/acschembio.1c00063
ACS Chem. Biol. XXXX, XXX, XXX−XXX